Master's thesis

NTNU
Norwegian University of Science and Technology
Faculty of Engineering
Department of Ocean Operations and Civil Engineering

Mingda Zhu

Genetic Algorithm-based Parameter Identification for Ship Manoeuvring Model under Wind Disturbance

Master's thesis in Ship Design
Supervisor: Houxiang Zhang
Co-supervisor: Guoyuan Li, Tongtong Wang
June 2021

NTNU
Norwegian University of
Science and Technology

Mingda Zhu

Genetic Algorithm-based Parameter Identification for Ship Manoeuvring Model under Wind Disturbance

Master's thesis in Ship Design
Supervisor: Houxiang Zhang
Co-supervisor: Guoyuan Li, Tongtong Wang
June 2021

Norwegian University of Science and Technology
Faculty of Engineering
Department of Ocean Operations and Civil Engineering

NTNU
Norwegian University of
Science and Technology

Abstract

With the rapid development in ship digitalization and automation, to accurately determine the ship mathematical model has become much more demanding. Dynamic ship mathematical model with high fidelity is the indispensable foundation to marine operations and innovations, enabling better operation, control and monitoring. It's an essential task to estimate the hydrodynamic coefficients under the environmental disturbances induced by the wind in order to establish a more realistic ship mathematical model. Parameter identification, as a useful tool, plays an outstanding role in the identification of ship mathematical model in manoeuvring. Identification methods such as the least square method, support vector machine method and genetic algorithm, are all restricted to their imperfection when using individually.

In this master thesis, an evolutionary optimization-based identification framework is proposed to combine the advantage of the identification method and optimization method. The parameter identification is conducted on the 3-DOF Abkowitz model of a Mariner cargo ship using data collected from zigzag simulation to obtain the hydrodynamic coefficients under various wind conditions. To study the effects of wind speed, noise and direction on the accuracy of identification results, three groups of experiments are carried out. Different patterns are summarized with regard to the corresponding effects of wind conditions. Identified hydrodynamic coefficients are verified by benchmark from PMM test and the model performance is further validated by trajectory and velocity comparison. The least square method + genetic algorithm and support vector machine method + genetic algorithm are able to improve the accuracy of some selected hydrodynamic coefficients by utilizing a global sensitivity analysis and they perform more effectively under certain scenarios which are specified in this thesis. However, the overall effectiveness and optimization efficiency of the framework needs to be further improved.

Preface

This thesis marks the final journey of my master career in Ship Design (now Naval Architecture) in Department of Ocean Operations and Civil Engineering at the Norwegian University of Science and Technology (NTNU). The passion of this research originates from the collaboration with researchers in our department in the project supported by Research Council of Norway. It's also one of my ambitions to make contribution to the ship industry. As the shipping world is marching into the new era of digitalization and automation, with more complicated missions and operations, the highly accurate mathematical model of ship is extremely necessary. It's my primary and ultimate goal to find out how to obtain a ship mathematical model in both effective and efficient way, and to develop useful tools to perform identification.

This work has been supervised by Prof. Houxiang Zhang, Prof. Guoyuan Li and PhD. Tongtong Wang from NTNU, to whom I would like to express my sincere gratitude for their guidance, suggestion, comment and feedback. They have been highly supportive to my work and providing me with huge confidence. Their strong creed of pursuing the best has been my greatest inspiration during the whole research period.

Acknowledgements

Foremost, the deepest appreciation is sent to my supervisor and co-supervisors, and without them, this work would never have been possible. I also would like to acknowledge those who played a role in my academic accomplishments. First of all, my parents, who have been motivating and enlightening with love and wisdom. They have been my brightest lighthouse when I sailed across the ocean of life. Then I would like to thank my classmate Rahul, who has been sharing the same high discipline with me and fighting along with me relentlessly for a better outcome. Furthermore, I would like to thank Mr. Ahmed Fawzy Gad, who has helped me a lot in programming in genetic algorithm with patience. In addition, many thanks to my colleagues, Chunlin Wang, Robert Skulstad, Peihua Han, Lars Ivar Hatledal and Motoyasu Kanazawa in Intelligent Systems Lab who have offered me help constantly in solving different problems and issues. Last but not least, I would like to thank my beloved girlfriend for always cheering me up and giving me courage to confront challenges whenever is needed.

Contents

List of Figures

List of Tables

Chapter 1

Introduction

Chapter 1 consists of three sections. Section one presents a complete background study of parameter identification and its great importance in numerous marine applications. In addition, with the challenges in parameter identification discussed, the motivation behind this research is brought forward as well as the limitation. In section two, the scope is narrowed down to the field of parameter identification of ship manoeuvring model and five research objectives regarding to the topic are established. Three scientific contributions of the master thesis are summarized in section three, which are linked with the research objectives. Last but not least, the outline of the master thesis is also given in last section.

1.1 Background and Motivation

In the course of maritime history, the determination of ship mathematical model has always been an essential task. With the accurate mathematical models, the abstraction of the physical structures can be well explained, which enables the further applications such as control and prediction. Nowadays, more and more intelligent ships are being built and speed of entering into the era of digitalization and automation are increasing. Undoubtedly, the demand for accurately determining the ship mathematical models will significantly grow so as to achieve the goal of better operation, control and monitoring. In addition to that, establishing reliable mathematical models is beneficial to both newly-built and commissioned vessels, which can provide a considerable economic value.

1.1.1 Parameter Identification in Marine Application

The most common way to identify a ship mathematical model is by estimating the hydrodynamic coefficients or parameters, which is often referred as parameter

identification. As a useful tool, parameter identification could be applied to various aspects of the maritime industry.

Parameter identification can provide solid support for establishment of ship's mathematical model in development of Digital Twin which is a novel concept proposed in recent years. Digital twin is a digitalization or virtual replication of a physical object or system, which consists of seven major components as shown in figure 1.1. One of the most critical elements in digital twin is mathematical model, such as analytical models and time-domain models. Consequently, for the sake of meeting the application requirement, it's necessary to develop a way where mathematical model with high fidelity and robustness can be efficiently determined.

Besides, it will facilitate the ship automation. Of all the latest innovations, ship automation is the one the most popular and complicated. As anticipated, the maritime future will also belong to automation, and autonomous ships will be the key players in the marine transportation, especially for cargos, oil and gas. Ambitious and challenging as it may seem, the foundation of autonomous shipping lies on the accurate modeling of the ship. It's a stage where parameter identification can play its part well. To a large extent, the whole concept depends upon the mathematical model of the ocean on-going vessel. Only when the adequate modelling is achieved, will the control, monitoring and navigation become possible.

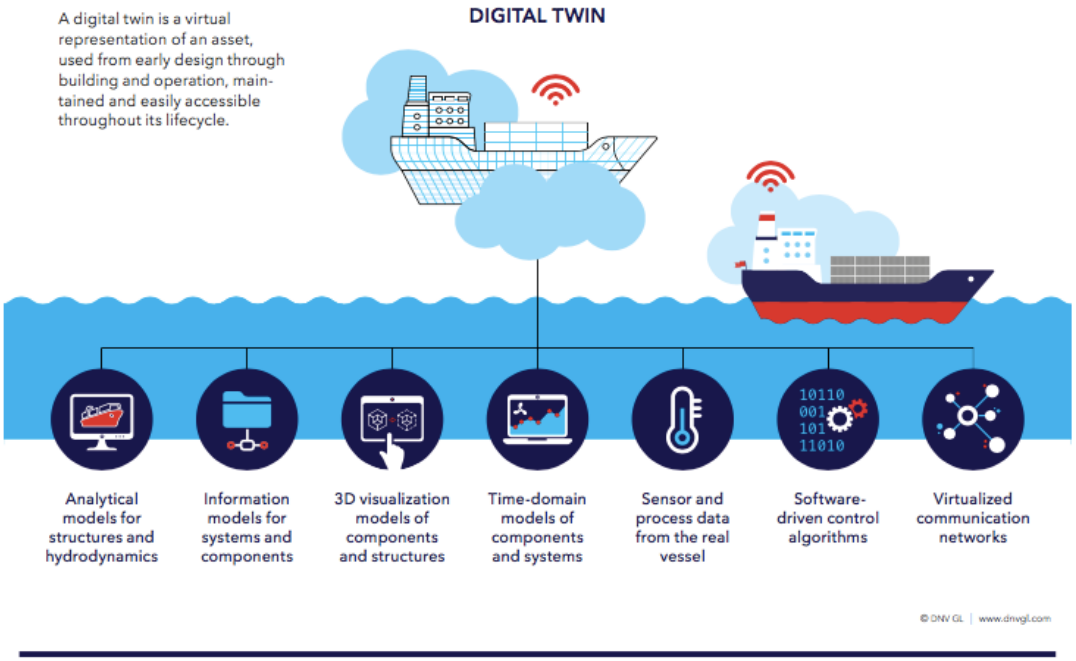

Figure 1.1: Structure of digital twin proposed by DNV GL [DNV, 2019]

In addition to marine innovations, the parameter identification of ship mathematical model has a great potential in increase of efficiency of sea trials. As known to many, sea trials are indispensable for the ship building industry, which usually take place on open water on full scale. Although the sea trials are generally considered to be performed only on the new-commissioned vessels, they are regularly conducted on vessels in service as well. The aim of sea trials is to measure the performance and seaworthiness of a vessel including speed, manoeuvrability, motion response and other important features, and as for the in-service vessels, influence due to any modifications may be investigated. Duration of the full-scaled sea trials varies from a few hours to several weeks, which will lead to reluctant cost for both shipyard and shipowner. It can make a difference in time reduction if the mathematical model of the vessel will come into play as an assistance and reference to the procedure. For instance, while conducting the manoeuvring trials , the hydrodynamic parameters are estimated and manoeuvring model of the ship is built up based on the data collected from various manoeuvres, Later, the model is put into computational simulation to generate the required manouvres for different test purposes and the trajectories can be then used as the reference for the actual ship behaviors. By taking this kind of measure, the working procedures can be simplified and repetitions for accuracy mitigated. Besides, the hydrodynamic parameters contain the essential information of physical properties of vessel, and they can be useful for sea trials of in-service vessels.

Parameter identification is also capable of calibration for commissioned vessel. Delivered in spring 2006, R/V Gunnerus, NTNU's research vessel, is equipped with the latest technology for a variety of research activities. During the last 15 years, several modifications have done to the vessel and the significant one was the elongation from 31.25 m to 35 m. As an extremely important educational platform for NTNU, the accurate mathematical modelling of Gunnerus is necessary and calibration is needed in which parameter identification can play a significant role to re-estimate the hydrodynamic coefficients and improve the model performance.

1.1.2 Challenges in Parameter Identification

In spite of the great possbile application of parameter identification, there are some inevitable challenges to meet, and limitation of the possible methods is one of them. Although there are several methods to carry out parameter identification such as experimental method, semi-empirical method, numerical method and system identification method, the former three more or less suffers from their inherent defects. For instance, experimental method is heavily dependent upon the standard manoeuvres of free-running tests which are both costly and time consuming. What's worse, the accuracy of the test results may be affected due to the uncertainties in the manoeuvres, imperfections of the experimental technique and

scaling effects.

System identification is an acknowledged approach used extensively in the research for its low experiment time and cost. It only requires state information and inertia terms without the need to measure the forces. What's more, it can be applied to full-scale vessel to avoid scale effects [Wang et al., 2019]. However, it might suffer from parameter drift and overfitting problems if there is noise in training data. Apart from that, collinearity problem in the complex structure of ship manoeuvring model cannot be eliminated, which will largely affect the accuracy and reliability of the hydrodynamic parameters, hence the mathematical model.

To improve the identification performance, many methods have been proposed and used in the system identification of ship manoeuvring model such as least square method, support vector machine, and genetic algorithm, but none of them is capable of solving the problems mentioned above single-handedly.

Environmental effect is one of the crucial factors to consider to improve the performance and robustness of the mathematical model in extreme conditions, but it's not easy to include all the components and many researches are carried out under calm water condition where environmental excitation forces and moments are neglected.

1.1.3 Research Motivation and Limitation

Parameter identification, as an effective tool, has a large potential of being implemented into the maritime industry if the accuracy, reliability and robustness are guaranteed. Therefore, to accomplish this mission, it's worthwhile to conduct research with regard to improvement of the identification efficiency and performance based on the existing methods. Moreover, there reminds a notable research gap in identification of ship manoeuvring model under environmental disturbances, such as wind, which also deserve more attention since it's an important millstone to reach on the way to obtain high-fidelity model.

Considering the resources and assistances available, the difficulties and duration of research, and the target to achieve, this master thesis will focus on the fundamental methods in parameter identification. Moreover, when it comes to environmental effect, only wind forces and moments will be taken into account in the identification process. Last but not least, simulation data will be used instead of real measurement data from sea trials or free-running tests.

1.2 Scope and Objective

The scope of this master thesis is the estimation of hydrodynamic parameters and identification of 3 degrees of freedom (3DOF) ship manoeuvring model using the system identification methods. The coverage will be within the content of ship manoeuvring where the corresponding principles shall be applied. It will mostly focus on the acknowledged mathematical models for ship manoeuvring such as Abkowitz model, and standard manoeuvres are selected for data generation where zig-zag manoeuvre is used extensively. Moreover, environmental forces such as wind forces and moments will be taken into account.

The research objectives of the master thesis can be listed as follows,

RO1 To estimate the hydrodynamic coefficients of target vessel using the simulation data under wind condition

RO2 To estimate the hydrodynamic coefficients using identification methods integrated with evolutionary optimization method under wind condition

RO3 To study effects of various important factors on the results, such as wind speed, measurement noise (in wind speed), wind direction

RO4 To conduct comparison study of the identified coefficients and system performances of ship model

RO5 To verify and validate the identified hydrodynamic coefficients and model using the benchmark from PMM test and manoeuvring simulation, respectively

1.3 Scientific Contribution and Outline

From the perspective of research, a master thesis should seek to make contribution to the scientific field and the development of technology. This work also aims for such target, and with its dedication to the parameter identification for ship model, the scientific contributions are summarized in the following contents:

SC1 Estimation of ship hydrodynamic coefficients under environmental disturbance induced by wind

SC2 Implementation of evolutionary optimization method to improve the accuracy of the estimated hydrodynamic coefficients and system performances

SC3 Analysis of the influences of several important factors on identification, including wind speed, measurement noise (in wind speed), wind direction

and the corresponding relation between scientific contributions and research objectives is shown in the table 1.1.

	SC1	SC2	SC3
RO1	*		
RO2		*	
RO3			*
RO4		*	*
RO5	*	*	*

Table 1.1: Relation between scientific contributions and research objetives

The rest of paper is organized as follows: Chapter 2 presents the literature review of the thesis. Methodology is introduced in Chapter 3, which includes the derivation of ship manoeuvring model and its identification form under wind disturbance, as well the the major components within evolutionary optimization-based identification framework. In Chapter 4, experiment setup of the thesis is described, and the identification results are analyzed and validated. Chapter 5 evaluates the proposed framework and discusses the environmental effect. In Chapter 6, the conclusion is summarized and future work is suggested.

Chapter 2

Literature Review

Literature review can be broken down into three parts. Section one starts with the review of parameter identification from the perspective of fundamental mathematical modeling, explaining the concept in a more detailed and comprehensive manner. Then, section two continues with the parameter identification in the field of ship manoeuvring by introducing the three most commonly used methods to estimate ship hydrodynamic coefficients and five acknowledged identification methods as well as two standard manoeuvres. Lastly, section three summarizes the current research status of parameter identification for ship manoeuvring model in terms of difficulty and deficiency.

2.1 Parameter Identification

Mathematical models, as opposed to physical models, mainly deal with the macroscopic scale of the dynamic system by solving the ordinary differential equations with finite dimension [Aarts, 2012]. In principle, there are two different ways to obtain a mathematical model of a real-world system: the theoretical one based on the derivation of the essential relationship of the dynamic system, and the empirical one, based on experiments on the dynamic system. It should be noted that practical approaches use a combination of both.

Difficulty in developing a mathematical model arises, when some of the important system parameters, or coefficients appearing in the model equations are unknown due to the complexity of the dynamic systems or insufficient amounts of operating data. The problem of lacking priori, can be solved by evaluating the data measured at the system input and output using parameter-identification methods through experiments with the real-world system, which is known as parameter identification. It is also defined as experimental detemination of values of parameters that govern the system behaviour in [Avula, 2003]. Parameter identification

is sometimes referred to as the inverse modelling problem, and general literature can be found in [H.T.Banks, 1989] and [Isakov, 1990]. One also encounters the alternative term parameter estimation.

Parameter-identification method can be stated as a link between data and models, where two workflows are often encountered, one is direct way and the other is indirect way by using an adjustable-parameter vector [Moeller, 2004]. The goal of any identification procedure is to obtain the unknown model parameters for the mathematical model. In practice, the identification procedures are often based on discrete measurements, and the identified model can be described in a continuous-time or discrete-time representation where the relation can be either linear or nonlinear.

2.2 Parameter Identification in Ship Manoeuvring

In the field of ship manoeuvring, parameter identification is the determination of hydrodynamic parameters or coefficients in the ship manoeuvring models using experimental data or measurement data through regression or other similar techniques. There are three prominent approaches to estimate the hydrodynamic parameters: experimental method, computational fluid dynamics (CFD) and system identification. Among them, system identification is the most popular one in the research. The data of control parameters such as rudder angle are measured and used as input, whereas the data of kinematic parameters such as speed and acceleration are measured and used as output. Then, by applying parameter identification methods such as least square method and support vector machine method with the data generating from manoeuvring simulation, one can obtain the hydrodynamic coefficients.

In the forthcoming subsections, the captive model test, CFD and system identification are introduced. Besides, Identification methods which are often employed in parameter identification of ship manoeuvring model are discussed along with two standard manoeuvres — turning circle and zigzag manoeuvre.

2.2.1 Captive Model Test

Captive model test is one of the most well-known experimental methods to measure the hydrodynamic force and moment for manoeuvring ships, which can be used to further estimate the hydrodynamic parameters. In the test, a scaled ship placed in the ship model basin is forced to move in a prescribed manner. Several captive model tests have been proposed to conduct the measurement such as oblique-towing test in a conventional long and narrow towing tank, rotating-arm test in a rotating-arm facility, the planar motion test using Planar Motion

Mechanism (PMM) in a long and narrow towing tank, as well as circular motion test (CMT) in a big towing tank. [Zaojian, 2006]

Among them, the planar motion test is the most widely used mainly because of the two distinct advantages it has. One is that planar motion test can fulfill the same mission as rotating arm test in a conventional long and narrow tank without using the expensive facility of rotating arm; The other one is that most of the hydrodynamic parameters can be determined using planar motion test which is often the reason why it's used to perform parameter identification [Xu et al., 2018a]. The captive model tests are likely to be subjected to scaling effects [Abkowitz, 1980], hence corrections are often needed and accuracy will be influenced.

2.2.2 Computational Fluid Dynamics (CFD)

Apart from captive model tests, numerical methods have been employed to calculate the hydrodynamic coefficients in recent years with the significant increase of the computational speed and steady development of new numerical solutions. CFD is a control volume method by solving Reynolds-Averaged Navier-Stokes (RANS) Equations. It is applied to calculate the hydrodynamic forces on a manoeuvring model taking into account the effects of dynamic sinkage in [Liu et al., 2019], while in [Islam and Guedes Soares, 2018], the estimation of hydrodynamic derivatives of a container ship is carried out by using PMM simulation performed in the OpenFOAM, an open-source RANS solver.

2.2.3 System Identification

One of the comprehensive definitions is given in the [Hayes, 1971], that in its most general form system identification is the process of properly mathematically modelling the behavior of a given system. The field of system identification uses statistical methods to build mathematical models of dynamical systems from measured data [Ljung, 1998], and the identification process is the determination, on the basis of input and output, of a system within a specified class of systems, to which the system under test is equivalent [Zadeh, 1962].

System identification is a very useful tool when it comes to the determination of the mathematical models of ship. Essentially, the purpose of system identification in the ship manoeuvring is to obtain a multiple regression model that reflects the characteristics of ship manoeuvring motion. The hydrodynamic coefficients in the regression model should be determined.

White-box, Black-box and Grey-box Modelling

The modeling approaches in the system identification can be categorized into three different kinds, which are white-box modelling, black-box modelling and grey-box modelling. They differ in the amount of physical relationships regarding of the model, where white-box is entirely based on the knowledge of physics, black-box is purely data-driven without the information and need for any priori, and grey-box is a combination of both requiring both measurement data and physical background. Considering the distinction on the priori knowledge included in the model, the grey-box modelling can be further classified into five branches: constrained black box identification, semi physical modelling, mechanistic modelling, hybrid modelling and distributed parameter modelling [Sohlberg and Jacobsen, 2008].

The selection of the approach is primarily dependent upon the priori available and the objective of the model to be built. White-box modelling, owing to the predominant fact that it requires outstanding physical insight into the model, can only be applied in the simple cases, hence not practical in the ship modeling problem. Black-box modelling, despite of the biggest shortcoming of being none-physical, could be quite remarkable in application when the main concern is the overall behavior or mapping of input-output relationship. One of the most significant examples of black-box modelling is artificial neutral network (ANN) which is one of the methods used extensively in the ship manoeuvring model identification. Compared with black-box modelling, grey-box is more flexible and robust as it includes the option to input some of known constraints such as parameters and noise. Besides, it can give an explicit interpretation to the dynamic model in terms of visual equations. Furthermore, coupling between parameters are likely to occur and grey-box modelling helps to specify the effect.

2.2.4 Identification Methods for Ship Model

The rich diversity in methods for parameter identification of ship manoeuvring model results in distinct complexity, which varies from simple measure to advanced algorithm. In this subsection, the most acknowledged approaches are reviewed, such as least square method, Kalman filter, genetic algorithm, support vector machine and artificial neural network.

Least Square Method

Least squares (LS) method is a classical and standard method for system identification. In [Ross et al., 2015], it is used to estimate hydrodynamic coefficients of R/V Gunnerus, the research vessel of Norwegian University of Science and Tech-

nology (NTNU), based on the data from PMM tests. Least square method is quite sensitive to noises and can be greatly influenced by the pollution of measurement data [Xu et al., 2018b], which could lead to non-consistent estimate [Söderström, 2013]. In [Chen and Ljung, 2013], a QR factorization based matrix-inversion-free algorithm is proposed in the regularized least-squares approach to deal with both large data sets and possibly ill-conditioned computations. An fast convergent iterative least square method is introduced in [Qin et al., 2014] to increase convergence speed and precision of the parameter identification. Partial least square (PLS) method is applied in [Jian-Chuan et al., 2015] and the evaluation of the performance of PLS regression shows its capability in processing measurement data with high dimensionality and heavy multicollinearity, especially in processing data with small sample size.

Kalman Filter

First developed in 1960 [Kalman, 1960], Kalman filter (KF) is a form of recursive least square estimation allowing the combination of information from a dynamic model and sensor measurement.In [Yoon and Rhee, 2003], an Estimation-Before-Modelling (EBM) technique, or two-step method, is introduced to identify the hydrodynamic coefficients for modified Abkowitz's model, where the extended Kalman filter and modified Bryson-Frazier (MBF) smoother are used to estimate the hydrodynamic forces and regression analysis is computed in the 2nd step.A method is proposed to carry out system identification for second-order modified Nomoto model for vessel steering in [Perera et al., 2015], and violent manoeuvres are performed to capture the nonlinear parameters of ocean going vessels under dynamic conditions. To deal with the shortcomings of extended Kalman filter methods, i.e., low precision and converge rate, the improved multi-innovation extended Kalman filter is proposed in [Xie et al., 2020], by introducing a forgetting factor to reduce cumulative effect of past interference.

Genetic Algorithm

Genetic algorithm is sometimes used for offline identification of ship manoeuvring model. In [Sutulo and Guedes Soares, 2014], an identification algorithm based on GA is developed and used to identify the 3DOF polynomial manoeuvring model. Several metrics have been tried in the minimization function of distance and to verify the identification algorithm, spiral manoeuvre and turning manoeure are performed.

Support Vector Machine

In the recent years, another type of machine learning method, Support Vector Machine (SVM), proposed by Vapnik [Boser et al., 1992] has been used to estimate the hydrodynamic coefficients for marine vessels. Compared with the ANN, the SVM is direct for finite samples and has a good generalization performance and global optimal extremum [Wang et al., 2013]. Least square support vector machine (LS-SVM) is a modified version of SVM proposed by [Suykens and Vandewalle, 1999]. In [Xu and Guedes Soares, 2016], LS-SVM is applied in parameter identification of two-dimensional path following control system, and an optimal truncated LS-SVM in [Xu and Soares, 2019] is used for hydrodynamic coefficient estimation of ship manoeuvring in shallow water. Support Vector Regression (SVR) [Drucker et al., 1997], which is the regression technique based on SVM, can be applied for parameter identification. It consists of the Least Square-SVR (LS-SVR), ϵ-SVR, υ-SVR etc. In [Zhang and Zou, 2011], an ϵ-SVR is used to identify the Abkowitz model for ship manoeuvring.

Artificial Neural Network

Artificial neural network(ANN) is another alternative approach to tackle identification of ship models. In [Luo and Zhang, 2016], a two-layer neural network is used to perform parameter identification for first order Nomoto model, and in [Rajesh and Bhattacharyya, 2008], an ANN is introduced to identify the nonlinear manoeuvring model of large tankers. Additionally, ANN is also used for curve-fitting and estimation for the rolling model of ship in [Mahfouz, 2004] and [Xing and McCue, 2010]. The ANN algorithms may have certain advantages as they do not imply any a priori structure of the ship mathematical model. But the absence of any physical ground behind the ANN model represents, at the same time, a natural disadvantage of ANN models as they cannot be extended, modified or tuned without full retraining which is not always possible [Sutulo and Guedes Soares, 2014].

2.2.5 Standard Manoeuvres

Standard manoeuvres are often used in the determination process of ship hydrodynamic parameters as the input siginal. In [Artyszuk, 2018], zigzag test is used for identification of the second-order linear Nomoto model and in [Xu and Guedes Soares, 2016], 20-20 zigzag simulation is generated for a known ship to provide data for parameter identification of the control model. Zigzag test and turning circle test are performed in [Shi et al., 2009] to both acquire data samples and verify the identified model.

According to The International Towing tank Conference (ITTC), there are in total 14 different types of full scale manoeuvring trials to test the 6 different manoeuvrabilities of vessel [ITTC, 2002]. The most commonly used ones are introduced in the following pages.

Turning Circle

Turning circle test can be used to evaluate the turning ability of ship performed to both port and starboard at approach speed with a maximum rudder angle. It is necessary to do a turning circle of at least 540 degrees to determine the main parameters of this trial including tactical diameter, advance, transfer, loss of speed on steady turn and velocity loss and time to change heading at 90 degrees, 180 degrees and 270 degrees. The main parameters and the path of the midship point are presented in figure 2.1.

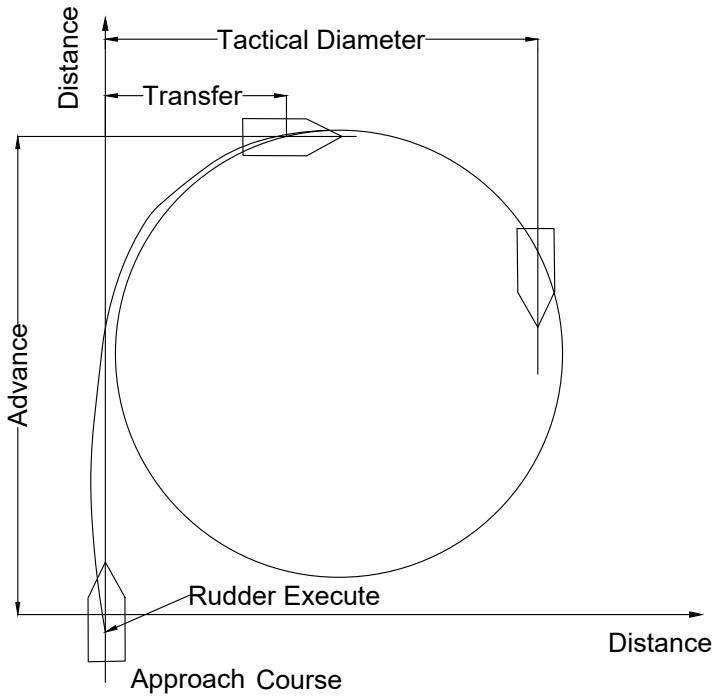

Figure 2.1: Turning circle. Adopted and modified from [ITTC, 2002]

Zig-zag Manoeuvre

The zigzag manoeuvre is obtained by reversing the rudder alternately by δ degrees to either side at a deviation of heading angle ψ from the initial course. After a steady approach the rudder is put over to starboard (first execute). When

the heading is ψ degrees off the initial course, the rudder is reversed to the same angle to port (second execute). After counter rudder has been applied, the ship initially continues yawing in the original direction with decreasing yaw rate until it changes sign, so that the ship eventually yaws to the left in response to the rudder. When the heading is ψ degrees off the course port, the rudder is reversed again to starboard (third execute). This process continues until a total of 3 rudder executes have been completed.

A zigzag manoeuvre is determined by the combination of the values of change of heading ψ and rudder angle δ, and is denoted $\delta/\ \psi$. Common values for these parameters are 10/10 and 20/20. Important parameters to obtain are: initial turning time, execute heading angle, overshoot angle, time to check yaw, heading, reach and time of a complete cycle.

For modified zigzag manoeuvre, the execute heading angle is as 1 degree and the rudder angle as 5 or 10 degrees while for ship at low speed, this manoeuvre is executed while the ship is running ahead by inertia after stopping the main engine. When the ship's speed drops below 5 knots, a 35/5 zigzag manoeuvre is initiated.

The time trace of zigzag manoeuvre parameters is shown in the figure 2.2.

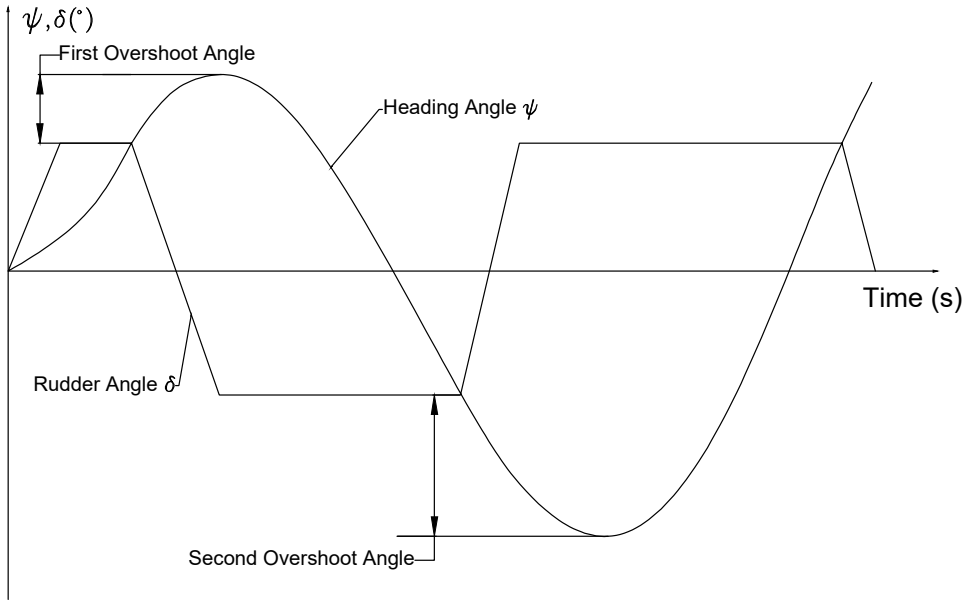

Figure 2.2: Zigzag Manoeuvre. Adopted and modified from [Yuan, 2017]

2.3 Summary and Critical Review

Parameter drift and overfitting are two significant problems that could be encountered in the research of parameter identification for ship manoeuvring, and the main reason behind is that the training data often contain noise. Parameter drift was first discovered by Hwang and in [Hwang, 1980], he applied parallel processing to process the training data but the results show that the problem still occurs. In [Araki et al., 2012], simulation results suggest the CFD simulation can reproduce the EFD free-running results, which is most accurate data source without measurement noise. Data pre-processing method is also proposed in [Luo and Li, 2017] such as the difference method and additional excitation method, and the results show that the parameter drift can be diminished by alleviating multicollinearity of the multiple regression models.

It was pointed out in [Perera et al., 2016] that zigzag and turning manoeuvres may fail to excite the nonlinear vessel steering parameters effectively, especially when there is a large number of parameters. In [Wang and Zou, 2018], Wang and Zou concluded that the collinearity is severe when dataset from a single standard manoeuvre is used as the training sample and datasets of different rudder angles induce different degree of collinearity, which might be due to different ship characteristics containing in them. In [Wang et al., 2019], to cope with the parameter drift problem, multiple standard manoeuvring datasets are applied simultaneously as the training data.

In spite of the use of global optimization algorithm in the parameter identification of ship manoeuvring model, it's often used together with SVM to determine the optimal hyper-parameters for SVM. In [Luo et al., 2016], particle swarm optimization is incorporated into SVM to obtain the optimized structural factors, and in [Xu and Guedes Soares, 2020], quantum-inspired evolutionary algorithm is used to search the optimal value of the predefined parameters of the nonlinear kernel-based LS-SVM. Very few has considered using evolutionary algorithm to optimize the identified hydrodynamic coefficients. Besides, one can also notice that in many researches, the calm water condition has been assumed while the environmental effects are often neglected, which might reduce the reliability of the mathematical model in real case. In [Wang et al., 2021], the environmental disturbances are modeled by means of Wiener process in the form of Gaussian white noise instead of considering the actual wind force and moment.

To sum up, the potential research gap lies on improvement in data-processing of input, more advanced simulation method to increase the richness of data, improvement of identification methodology by combining two or more possible methods, and identification under wind disturbances with more accurate modeling, and the latter two is what this thesis aims to fill in and make contribution to.

Chapter 3

Methodology

This chapter is divided into two sections. The first section introduces the mathematical modelling of ship manoeuvring which includes kinematics, dynamics, and wind forces and moments; the second section discusses the evolutionary optimization-based identification framework which contains data generation, identification methods, sensitivity analysis and genetic algorithm.

3.1 Ship Manoeuvring Modelling

In the realm of Naval Architecture, there are large varieties of models developed for different purposes such as prediction, real-time simulation and controller-observer design and in [Fossen, 2011], they are classified into mainly three types: simulation model, control design model, and observer design model. Simulation model is the most accurate description of a system, which includes the ship dynamics, propulsion system, measurement system and the environmental forces due to wind, waves and ocean currents. This way of modeling can be adopted and modified in the programming software, e.g. Matlab.

The scope of this master thesis is within ship manoeuvring, therefore it's necessary to recap the fundamental theories of it. According to [Fossen, 2011], ship manoeuvring is the study of a ship moving at constant positive speed in restricted calm water based on the assumption that the manoeuvring or hydrodynamic coefficients are frequency independent. The assumption of frequency independent indicates that there will be a zero-frequency wave excitation such that added mass and damping can be represented by using hydrodynamic derivatives or constant parameters. One important point to notice is that the frequency independent assumption is only valid for surge, sway and yaw motion as the natural frequency of ship is close to zero. As a consequence of this, the ship manoeuvring model is usually formulated as a coupled surge-sway-yaw model neglecting the other three

motions.

3.1.1 Kinematics of Ship Motion

Kinematics considers only the geometry of motion without presence of mass and forces which is decomposed into motion variables and reference frames.

Motion Variables

Marine vessels operates in six degrees of freedom (6 DOFs), thus six independent coordinates are needed to determine the position and orientation. The first three coordinates, and their time derivatives, correspond to the position and translational motion along the x, y and z axes, while the last three coordinates and their time derivatives are used to describe orientation and rotational motion. For marine vessels, the six different motion components are defined as surge, sway, heave, roll, pitch and yaw (see figure 3.1). The table of notation for marine vessels defined by Society of Naval Architects and Marine Engineers (SNAME) is presented in table 3.1.

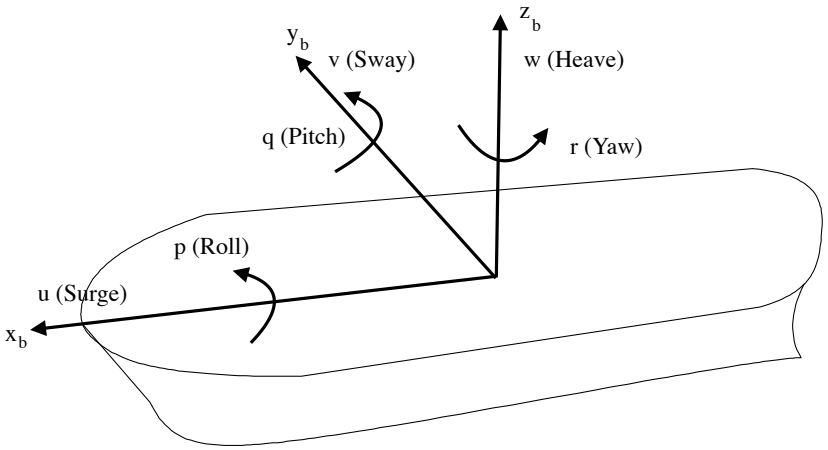

Figure 3.1: Illustration of motion variables for a marine vessel

DOF		Forces and moments	Linear and angular velocities	Positions and Euler angles
1	motions in the x direction (surge)	X	u	x
2	motions in the y direction (sway)	Y	v	y
3	motions in the z direction (heave)	Z	w	z
4	rotation about the x axis (roll, heel)	K	p	ϕ
5	rotation about the y axis (pitch, trim)	M	q	θ
6	rotation about the z axis (yaw)	N	r	ψ

Table 3.1: The notation of SNAME [SNAME, 1950] for marine vessels.

Reference Frames

In general, two types of reference frames could be defined, namely Earth-centered coordinate frames and geographic reference frames. The Earth-centered coordinate frames could be further divided into the Earth-centered inertial frame and the Earth-centered Earth-fixed frame, and the geographic reference frames are comprised of the North-East-Down coordinate system and the body-fixed coordinate system.

ECI The Earth-centered inertial (ECI) frame, denoted as {i}, is a non-rotating frame with its origin fixed at earth's center and falls freely along with the earth in the gravitational fields of the other solar system bodies [Rizzi and Ruggiero, 2013].

ECEF The Earth-centered Earth-fixed (ECEF) reference frame, denoted as {e}, in contrast to the ECI, rotates with the earth with its axes aligned with the international reference pole (IRP), international reference meridian (IRM) and true North, respectively.

NED The North-East-Down (NED) coordinate system, denoted as {n}, is a coordinate system fixed to the Earth's surface. The origin is arbitrarily fixed to a point on the Earth's surface with the X-axis pointing toward the ellipsoid north (geodetic north), the Y-axis pointing toward the ellipsoid east (geodetic east) and the Z-axis pointing downward along the ellipsoid normal [Cai et al., 2011].

BODY The body-fixed coordinate system, denoted as {b}, is a vehicle-carried carried coordinate system with its origin defined on the body of the vessel. The position and orientation of the vessel are described relative to the inertial reference frame (approximated by {e} or {n} for marine vessel) while the linear and angular velocities of the craft should be expressed in the body-fixed coordinate system.

3.1.2 Dynamics of Ship Manoeuvring

Dynamics, as opposed to kinematics, deal with forces and their relation primarily to motion. Here, the dynamics is addressed from two aspects: derivation of ship manoeuvring model and Abkowitz model.

Derivation of Ship Manoeuvring Model

To formulate the dynamic equation for ship manoeuvring motion, an earth-fixed coordinate system (x_0, y_0) is introduced with the origin being the position of center of gravity (CG) at time t_0 and the the body-fixed coordinate system (x, y) is defined to move together with the ship, as shown in figure 3.2. Both x axis and x_0 axis points to the direction of original course with z and z_0 pointing downwards vertically. The angle between the directions of x_0 axis and x axis is defined as the heading angle, ψ.

The manoeuvring motion of the ship in the horizontal plane is described by the speed $\vec{V}$ of translational motion and the yaw rate r $= \dot{\psi}$ of rotational motion about the z axis. The speed $\vec{V}$ can be decomposed into u and v in the x and y axis, respectively. The drift angle β is defined as the angle between direction of speed $\vec{V}$ and x axis. Therefore,

$$u = Vcos\beta, v = -Vsin\beta, V = |\vec{V}| \tag{3.1}$$

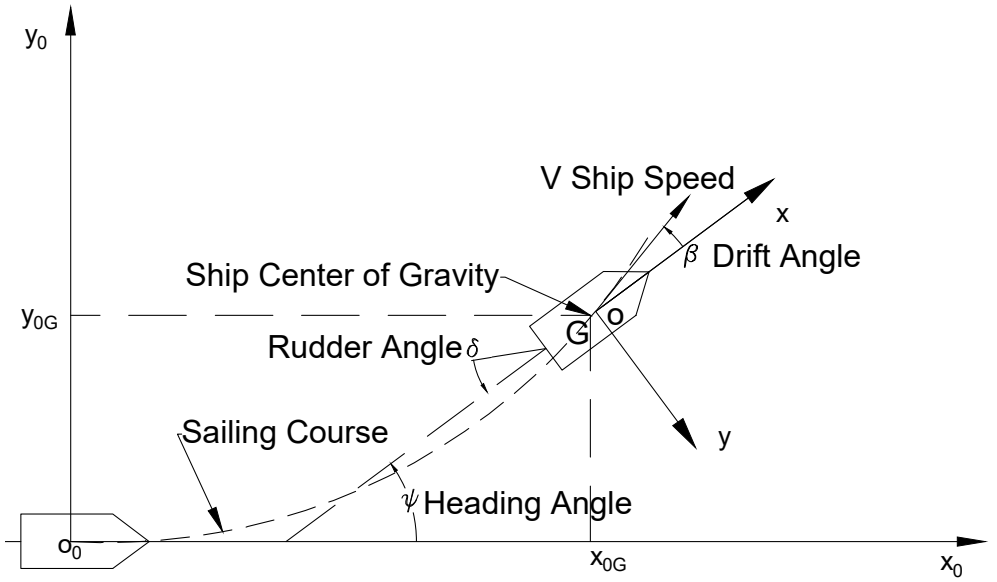

Figure 3.2: Description of coordinate system. Adopted and modified from [Zaojian, 2006]

Then, by applying Newton's 2nd law, the equations of motion in earth-fixed coordinate system can be obtained as follows,

$$\begin{aligned} X_0 &= m\ddot{x}_{oG} \\ Y_0 &= m\ddot{y}_{oG} \\ N_0 &= I_{zG}\ddot{\psi} \end{aligned} \tag{3.2}$$

and by utilizing the relationship of the external forces and moment between earth-fixed and body-fixed coordinate system, the equations of motion can be expressed in the body-fixed coordinate system, as shown in the Equation (3.3).

$$\begin{aligned} X &= m(\dot{u}_G - v_G\dot{\psi}) \\ Y &= m(\dot{v}_G + u_G\dot{\psi}) \\ N &= I_{zG}\ddot{\psi} \end{aligned} \tag{3.3}$$

In practice, the origin of body-fixed coordinate system is assumed to be on the midship point instead of on the center of gravity (x_G, 0, z_G), hence the equations of motion in the body-fixed coordinate system with the original of the coordinate system lying on the midship point are finally formulated in the following,

$$\begin{aligned} m(\dot{u} - vr - x_G r^2) &= X \\ m(\dot{v} + ur + x_G\dot{r}) &= Y \\ I_z\dot{r} + mx_G(\dot{v} + ur) &= N \end{aligned} \tag{3.4}$$

where I_z is the moment of inertia about z axis and r = $\dot{\psi}$ is the yaw rate about the z axis

Abkowitz Model

There are several ways to express hydrodynamic forces and moments in the mathematical model of ship manoeuvring, which results in different model structures. The selection of model structure is a trade-off between model complexity and model capacity. In the present paper, the 3DOF Abkowitz model of a Mariner class cargo vessel is taken as a case study. The model structure is modified based on [Chislett and Strom-Tejsen, 1965], and some revisions have been made by Fossen [Fossen and Perez, 2004]. The hydrodynamic force and moment are expressed as functions of kinematical parameters and rudder angle and by applying a third-order truncated Taylor-series expansion to the functions with the assumptions made, which yields the three equations as shown in Equation (3.5). There are in total 40 coefficients with 10 in surge motion, 15 in sway motion and 15 in yaw motion, respectively.

$$
\begin{aligned}
X &= X_{\dot{u}}\dot{u} + X_u\Delta u + X_{uu}\Delta u^2 + X_{uuu}\Delta u^3 + X_{vv}v^2 + X_{rr}r^2 + X_{rv}rv + X_{\delta\delta}\delta^2 \\
&\quad + X_{u\delta\delta}\Delta u\delta^2 + X_{v\delta}v\delta + X_{uv\delta}\Delta uv\delta \\
Y &= Y_v v + Y_r r + Y_{vvv}v^3 + Y_{vvr}v^2 r + Y_{vu}v\Delta u + Y_{ru}r\Delta u + Y_\delta\delta + Y_{\delta\delta\delta}\delta^3 + Y_{u\delta}\Delta u\delta \\
&\quad + Y_{uu\delta}\Delta u^2\delta + Y_{v\delta\delta}v\delta^2 + Y_{vv\delta}v^2\delta + Y_0 + Y_{0u}u + Y_{0uu}u^2 \\
N &= N_v v + N_r r + N_{vvv}v^3 + N_{vvr}v^2 r + N_{vu}v\Delta u + N_{ru}r\Delta u + N_\delta\delta + N_{\delta\delta\delta}\delta^3 + N_{u\delta}\Delta u\delta \\
&\quad + N_{uu\delta}\Delta u^2\delta + N_{v\delta\delta}v\delta^2 + N_{vv\delta}v^2\delta + N_0 + N_{0u}u + N_{0uu}u^2
\end{aligned}
\tag{3.5}
$$

The forces and moments on the right-hand side of Equation (3.4) can be expressed in non-dimensional form:

$$
\begin{aligned}
X &= \frac{1}{2}\rho L^2 U^2 X' \\
Y &= \frac{1}{2}\rho L^2 U^2 Y' \\
N &= \frac{1}{2}\rho L^3 U^2 N'
\end{aligned}
\tag{3.6}
$$

where ρ is the density of water, L is the ship length, U $= \sqrt{(U_0 + \Delta u)^2 + v^2}$ is the instantaneous ship speed, Δu is perturbed surge velocity about nominal speed U_0, which is equivalent to the notation u in [Fossen and Perez, 2004]. For convenience, u is adopted in the following expressions.

Rewriting Equation (3.4) in a non-dimensional form and substituting non-dimensional form of Equation (3.5) into it, the following terms are obtained:

$$
\begin{aligned}
(m' - X'_{\dot{u}})\dot{u}' &= f_1(u, v, r, \delta)' \\
(m' - Y'_{\dot{v}})\dot{v}' + (m'x'_G - Y'_{\dot{r}})\dot{r}' &= f_2(u, v, r, \delta)' \\
(m'x'_G - N'_{\dot{v}})\dot{v}' + (I'_z - N'_{\dot{r}})\dot{r}' &= f_3(u, v, r, \delta)'
\end{aligned}
\tag{3.7}
$$

where f_1, f_2 and f_3 are modified Abkowitz equations in non-dimensional form related to state variables as shown in Equation (3.8); $X'_{\dot{u}}$, $Y'_{\dot{v}}$, $Y'_{\dot{r}}$, $N'_{\dot{v}}$ and $N'_{\dot{r}}$ are non-dimensional added mass coefficients.

$$
\begin{aligned}
f_1(u,v,r,\delta)' &= X'_u u' + X'_{uu} u'^2 + X'_{uuu} u'^3 + X'_{vv} v'^2 + X'_{rr} r'^2 + X'_{rv} r' v' + X'_{\delta\delta}\delta^2 \\
&\quad + X'_{u\delta\delta} u' \delta^2 + X'_{v\delta} v'\delta + X'_{uv\delta} u' v' \delta \\
f_2(u,v,r,\delta)' &= Y'_v v' + Y'_r r' + Y'_{vvv} v'^3 + Y'_{vvr} v'^2 r' + Y'_{vu} v' u' + Y'_{ru} r' u' + Y'_\delta \delta + Y'_{\delta\delta\delta}\delta^3 \\
&\quad + Y'_{u\delta} u'\delta + Y'_{uu\delta} \Delta u'^2 \delta + Y'_{v\delta\delta} v' \delta^2 + Y'_{vv\delta} v'^2 \delta + Y'_0 + Y'_{0u} u' + Y'_{0uu} u'^2 \\
f_3(u,v,r,\delta)' &= N'_v v' + N'_r r' + N'_{vvv} v'^3 + N'_{vvr} v'^2 r' + N'_{vu} v' u' + N'_{ru} r' u' + N'_\delta \delta + N'_{\delta\delta\delta}\delta^3 \\
&\quad + N'_{u\delta} u'\delta + N'_{uu\delta} u'^2 \delta + N'_{v\delta\delta} v' \delta^2 + N'_{vv\delta} v'^2 \delta + N'_0 + N'_{0u} u' + N'_{0uu} u'^2
\end{aligned}
\tag{3.8}
$$

where hydrodynamic derivatives $\{X_{(.)}, Y_{(.)}, N_{(.)}\}$ are parameters to be identified.

To derive the identification model, the Euler's Stepping method is used. In this way, the accelerations are expressed in terms of velocities difference and the equations are discretized. Δt below is the time interval.

$$
\begin{aligned}
u(k+1) - u(k) &= \dot{u}(k)\Delta t \\
v(k+1) - v(k) &= \dot{v}(k)\Delta t \\
r(k+1) - r(k) &= \dot{r}(k)\Delta t
\end{aligned}
\tag{3.9}
$$

Let $m_{11} = m' - X'_{\dot{u}}$, $m_{22} = m' - Y'_{\dot{v}}$, $m_{23} = m'x'_G - Y'_{\dot{r}}$, $m_{32} = m'x'_G - N'_{\dot{v}}$, $m_{33} = I'_z - N'_{\dot{r}}$, the identification model can be written in matrix form:

$$
\begin{aligned}
\frac{u(k+1)-u(k)}{\Delta t} m_{11} &= AX(k) \\
\frac{v(k+1)-v(k)}{\Delta t} m_{22} + \frac{r(k+1)-r(k)}{\Delta t} m_{23} &= BY((k) \\
\frac{v(k+1)-v(k)}{\Delta t} m_{32} + \frac{r(k+1)-r(k)}{\Delta t} m_{33} &= CN(k)
\end{aligned}
\tag{3.10}
$$

where A, B, C are constant parameter vectors to be identified which correspond to hydrodynamic derivatives mentioned above, and $X(k)$, $Y(k)$, $N(k)$ are input vectors. The input vectors and parameter vectors can be written as:

$$
\begin{aligned}
X(k) =& [u'(k), u'(k)^2, u(k)^3, v'(k)^2, r'(k)^2, r'(k)v'(k), \delta(k)^2, u'(k)\delta(k)^2, \\
& v'(k)\delta(k), u'(k)v'(k)\delta(k)] \\
Y(k) =& [v'(k), r'(k), v'(k)^3, v'(k)^2 r'(k), v'(k)u'(k), r'(k)u'(k), \delta(k), \delta(k)^3, u'(k)\delta(k), \\
& u'(k)^2\delta(k), v'(k)\delta(k)^2, v'(k)^2\delta(k), 1, u'(k), u'(k)^2] \\
N(k) =& [v'(k), r'(k), v'(k)^3, v'(k)^2 r'(k), v'(k)u'(k), r'(k)u'(k), \delta(k), \delta(k)^3, u'(k)\delta(k), \\
& u'(k)^2\delta(k), v'(k)\delta(k)^2, v'(k)^2\delta(k), 1, u'(k), u'(k)^2]
\end{aligned}
\tag{3.11}
$$

$$\begin{aligned} A &= [a_1, a_2 \cdots a_{10}] \\ B &= [b_1, b_2 \cdots b_{15}] \\ C &= [c_1, c_2 \cdots c_{15}] \end{aligned} \tag{3.12}$$

The transformation between non-dimensional velocity and dimensional velocity can be expressed as:

$$\begin{aligned} u' &= \frac{u}{U} \\ v' &= \frac{v}{U} \\ r' &= \frac{rL}{U} \end{aligned} \tag{3.13}$$

It should be noticed here that the non-dimensional mass and added mass coefficients are treated as priori knowledge, which can be normally estimated using strip theory or empirical formulas.

3.1.3 Wind Force and Moment

Let V_w, β_w, γ_w, V_{rw} denote the wind speed, direction, attack angle and relative wind speed, respectively(see Figure 3.3). For a ship moving at a forward speed, the wind force and moment in surge, sway and yaw can be defined as follows,

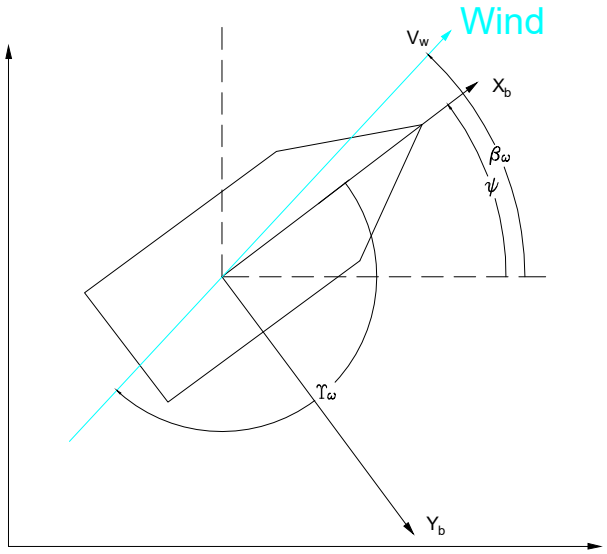

Figure 3.3: Sketch of wind on marine vessel

$$\tau_{wind} = \frac{1}{2}\rho_a V_{rw}^2 \begin{bmatrix} C_X(\gamma_{rw})A_{Fw} \\ C_Y(\gamma_{rw})A_{Lw} \\ C_N(\gamma_{rw})A_{Lw}L_{oa} \end{bmatrix} \tag{3.14}$$

with

$$V_{rw} = \sqrt{u_{rw}^2 + v_{rw}^2} \tag{3.15}$$

$$\gamma_{rw} = -atan2(v_{rw}, u_{rw}) \tag{3.16}$$

The relative velocities are

$$\begin{aligned} u_{rw} &= u + u_w \\ v_{rw} &= v - v_w \end{aligned} \tag{3.17}$$

where

$$\begin{aligned} u_w &= V_w cos(\beta_w - \psi) \\ v_w &= V_w sin(\beta_w - \psi) \end{aligned} \tag{3.18}$$

Applying the load concept developed by [Blendermann, 1994], the wind coefficients are expressed as:

$$\begin{aligned} C_X(\gamma_w) &= -CD_l \frac{A_{Lw}}{A_{Fw}} \frac{cos(\gamma_w)}{1 - \frac{\delta}{2}(1 - \frac{CD_l}{CD_t})sin^2(2\gamma_w)} \\ C_Y(\gamma_w) &= CD_t \frac{sin(\gamma_w)}{1 - \frac{\delta}{2}(1 - \frac{CD_l}{CD_t})sin^2(2\gamma_w)} \\ C_N(\gamma_w) &= [\frac{s_L}{L_{oa}} - 0.18(\gamma_w - \frac{\pi}{2})]C_Y(\gamma_w) \end{aligned} \tag{3.19}$$

where A_{Lw} is lateral projected area, A_{Fw} is frontal projected area, CD_l is longitudinal resistance, CD_t is transverse resistance, δ is the cross-force, L_{oa} is the ship length and s_L is the horizontal distance from amidships section to centre of lateral projected area. Coefficients of lateral, longitudinal resistance and cross-force can be obtained from the table in [Blendermann, 1994], while ship-related parameters such as A_{Lw}, A_{Fw} and s_L can be approximated using the data sample in [Fujiwara and Nimura, 2005] with similar size to Mariner class cargo ship.

With wind force and moment, the Equation (3.4) becomes,

$$\begin{aligned} m(\dot{u} - vr - x_G r^2) &= X + \tau_x \\ m(\dot{v} + ur + x_G \dot{r}) &= Y + \tau_y \\ I_z \dot{r} + m x_G(\dot{v} + ur) &= N + \tau_n \end{aligned} \tag{3.20}$$

and the identification model becomes,

$$\begin{aligned} \frac{u(k+1) - u(k)}{\Delta t} m_{11} &= AX(k) - \tau'_x \\ \frac{v(k+1) - v(k)}{\Delta t} m_{22} + \frac{r(k+1) - r(k)}{\Delta t} m_{23} &= BY((k) - \tau'_y \\ \frac{v(k+1) - v(k)}{\Delta t} m_{32} + \frac{r(k+1) - r(k)}{\Delta t} m_{33} &= CN(k) - \tau'_n \end{aligned} \tag{3.21}$$

where τ'_x, τ'_y and τ'_n are the non-dimensional forms of wind force and moment in surge, sway and yaw motion, respectively.

3.2 Evolutionary Optimization-based Identification Framework

From the previous studies, it's not difficult to find out that almost all the identification methods have their thresholds. Least square method (LS) suffers from measurement noise problem; support vector machine method (SVM) has difficulty finding the optimal values of hyper-parameters and genetic algorithm (GA) requires priori knowledge of the hydrodynamic coefficients for initiation. Therefore, the identification method + evolutionary optimization framework is proposed here to combine the strength of system identification methods with that of global optimization method. To make it more generic, two identification methods are selected for this paper as well as one optimization method, all of which can be considered as fundamental approach in their individual field and more importantly, are easy to implement. Furthermore, sensitivity analysis (SA) is employed to group the identified hydrodynamic coefficients to enhance the efficiency of optimization process. Last but not least, data generation method is described with some basic assumptions made. The flowchart of the framework is shown in figure 3.4.

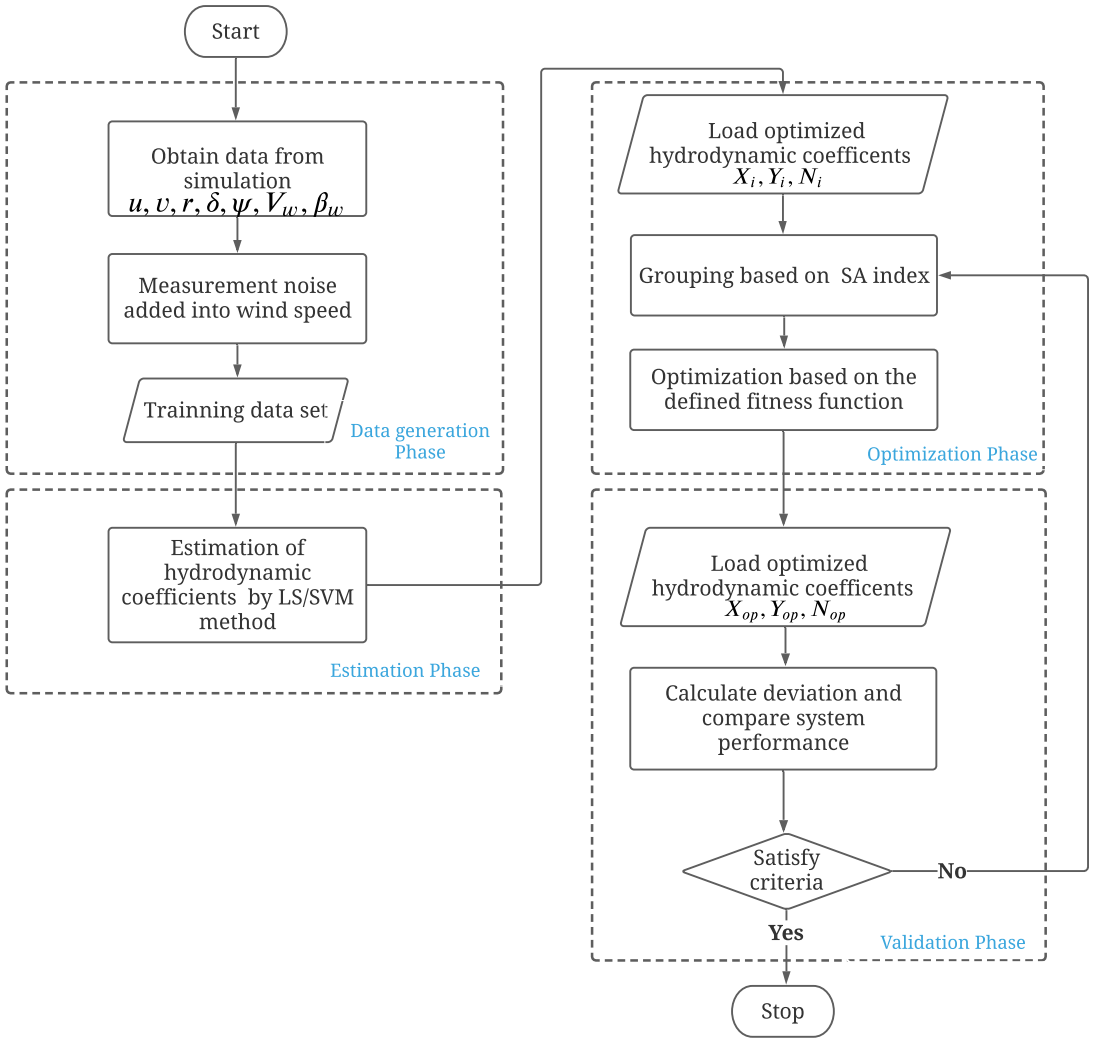

Figure 3.4: Flowchart of evolutionary optimization-based identification framework

3.2.1 Data Generation

In reality, data is mostly collected from ship onboard sensors, which inevitably contains measurement noise and environmental disturbance. The measurement noise, as discussed above, will cause problems such as parameter drift, which leads to large inaccuracy of the identified hydrodynamic coefficients. Even though the motions generated from the manoeuvring model built with those less precise coefficients may have good agreement with the training data, the generalization can't be promised when the collinearity is severe. In spite of many researches devoted into solutions to such problems, the effect of parameter drift can't be eliminated

for measurement data from sensors. Therefore, the parameter identification is challenging to achieve under the intervention of measurement noise.

What this paper ultimately aims for is to identify hydrodynamic coefficients using the proposed identification and evolutionary optimization framework under wind disturbance, for which the measurement noise in the input variables such as ship speed components and rudder angle is assumed to be neglected while keeping only the measurement noise in the wind speed.

3.2.2 Identification Methods

LS method

The Least square method is a standard approach in regression analysis to approximate the solution of overdetermined system by minimizing the sum of the squares of errors made in the results of every single equation. Given an overdetermined system as shown in Equation (3.22) of m linear equations in n unknown coefficients, with m>n, the matrix form can be written as,

$$\sum_{l=1}^{n} X_{kl}\beta_l = y_k, (k = 1, 2, ..., m) \tag{3.22}$$

$$\mathrm{X}\boldsymbol{\beta} = \mathbf{y} \tag{3.23}$$

where

$$\mathrm{X} = \begin{bmatrix} X_{11} & X_{12} & \cdots & X_{1n} \\ X_{21} & X_{22} & \cdots & X_{2n} \\ \vdots & \vdots & \ddots & \vdots \\ X_{m1} & X_{m2} & \cdots & X_{mn} \end{bmatrix}, \qquad \boldsymbol{\beta} = \begin{bmatrix} \beta_1 \\ \beta_2 \\ \vdots \\ \beta_n \end{bmatrix}, \qquad \mathbf{y} = \begin{bmatrix} y_1 \\ y_2 \\ \vdots \\ y_m \end{bmatrix} \tag{3.24}$$

As a rule, he constant term is always included in the set of regressors X with the first column X_{k1} (k=1, ..., m) filled with ones, and the coefficient β_1 corresponding to this regressor is called the intercept.

In practice, only an approximate solution can be found, for which quadratic minimization problem needs to be solved,

$$\hat{\boldsymbol{\beta}} = \arg\min_{\boldsymbol{\beta}} S(\boldsymbol{\beta}) \tag{3.25}$$

where the objective function S is given by

$$S(\boldsymbol{\beta}) = \sum_{i=1}^{n} \left| y_i - \sum_{j=1}^{p} X_{ij}\beta_j \right|^2 = \left\| \mathbf{y} - \mathrm{X}\boldsymbol{\beta} \right\|^2 \tag{3.26}$$

The minimization problem has a unique solution if and only if X has k linearly independent columns. By solving the normal equations,

$$(\mathrm{X}^\intercal \mathrm{X})\hat{\boldsymbol{\beta}} = \mathrm{X}^\intercal \mathbf{y} \tag{3.27}$$

the coefficient vector $\hat{\boldsymbol{\beta}}$ is obtained as:

$$\hat{\boldsymbol{\beta}} = \left(\mathrm{X}^\intercal \mathrm{X}\right)^{-1} \mathrm{X}^\intercal \mathbf{y} \tag{3.28}$$

SVM method

In machine learning, support vector machines are supervised learning models that can be used for classification and regression analysis. Suppose the training data sets $\mathrm{S} = \{s_k | s_k = (x_k, y_k), x_k \in \mathbb{R}^n, y_i \in \mathbb{R}\}_{k=1}^m$, the general approximation function of SVM is given:

$$\mathbf{y}(x) = \mathbf{w}^T \phi(x) + b \tag{3.29}$$

where x is the input, $\mathbf{y}(x)$ are the target values, $\mathbf{w}$ is a weight matrix, $\phi(x)$ is mapping function that map the input data to a higher dimensional feature space. The least squares version of SVM regressor is obtained by reformulating the minimization problem in the primal weight space as:

$$\underset{w,b,e_k}{min} J(w,e) = \frac{1}{2}\mathbf{w}^T\mathbf{w} + \frac{1}{2}C\sum_{k=1}^{m} e_k^2 \tag{3.30}$$

subject to

$$\mathbf{y}_k = \mathbf{w}^T\phi(x_k) + b + e_k, \qquad k = 1, ..., m \tag{3.31}$$

where e_k is the error and C is the regularization factor which represents the trade-off between model accuracy and model complexity.

The solution is obtained by constructing the Lagrangian function:

$$L(\mathbf{w}, b, e_k, a_k) = \frac{1}{2}\mathbf{w}^T\mathbf{w} + \frac{1}{2}C\sum_{k=1}^{n} e_k^2 - \sum_{k}^{n} \alpha_k[\mathbf{w}^T\phi(x_k) + b + e_k - \mathbf{y}_k] \tag{3.32}$$

where $\alpha_k \in \mathbb{R}$ are the Lagrangian multipliers. The conditions for optimality are shown in Equation (3.33) based on Karush-Kuhn-Tucker conditions (KKT) [Suykens et al., 2002]:

$$\begin{cases} \frac{\partial L}{\partial \mathbf{w}} = 0 & \rightarrow \quad \mathbf{w} = \sum_{k=1}^{m} \alpha_i \phi(x_k), \\ \frac{\partial L}{\partial b} = 0 & \rightarrow \quad \sum_{k=1}^{m} \alpha_m = 0, \\ \frac{\partial L}{\partial e_k} = 0 & \rightarrow \quad \alpha_k = C e_k, \ k = 1, \ldots, m, \\ \frac{\partial L}{\partial \alpha_k} = 0 & \rightarrow \quad y_k = \mathbf{w}^T \phi(x_k) + b + e_k, \ k = 1, \ldots, m. \end{cases} \tag{3.33}$$

Elimination of $\mathbf{w}$ and e will yield the following solution:

$$\begin{bmatrix} 0 & 1_m^T \\ 1_m & K(x_i, x_j) + C^{-1} I_m \end{bmatrix} \begin{bmatrix} b \\ \alpha \end{bmatrix} = \begin{bmatrix} 0 \\ Y \end{bmatrix}, \tag{3.34}$$

where I_m is an $N \times N$ identity matrix, $\alpha = [\alpha_1, \ldots, \alpha_m]^T$, $Y = [y_1, \ldots, y_m]^T$, $1_m = [1, \ldots, 1]^T$ and $K(x_i, x_j)$ is the kernel function. The kernel function is defined by :

$$K(x_h, x_k) = \phi(x_h)^T \phi(x_k), \ k = 1, ..., m \tag{3.35}$$

and the resulted SVM model for regression is obtained as :

$$\mathbf{y}(x) = \sum_{k=1}^{m} \alpha_k K(x \cdot x_k) + b \tag{3.36}$$

Estimation Procedure

When the simulation data is available, linear regression using either LS or SVM method can be conducted on the identification model derived in Equation (3.10) and (3.21) to estimate the parameters and intercept, which are in fact the hydrodynamic coefficients in its original form. With the hydrodynamic coefficients identified and ship behaviour information such as trajectories and velocities entered as input, the next step can be started. At the same time, the hydrodynamic coefficients can be also used to compute manoeuvring model for generalization performance comparison which later is used for validation. The estimation procedure of this paper illustrating the first two phases of figure 3.4 in details is given in Figure 3.5.

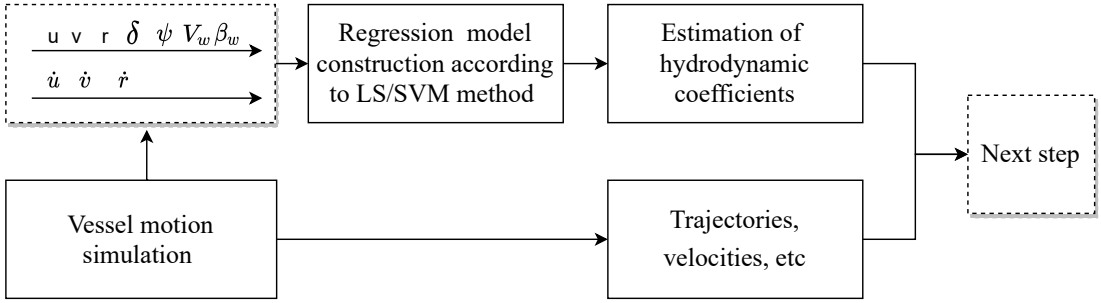

Figure 3.5: Estimation procedure

3.2.3 Sensitivity Analysis

Sensitivity analysis is the study of how the uncertainty in the output of a model can be apportioned to different sources of uncertainty in the model [Saltelli, 2002]. The global sensitivity analysis is able to provide importance ranking for the input according to the sensitivity index computed based on Monte Carlo simulation, which in turn gives indication to the relative importance of corresponding parameters.

Knowing that it's not practical to optimize 40 coefficients simultaneously, a global sensitivity method Sobol is introduced in this paper. The Sobol method is a variance-based sensitivity analysis method, which has been widely used in many disciplines. Assuming the model form is $f(x) = f(x_1, ..., f_M)$, where $X = (x_1, ..., x_M)$ represents the model input containing M independent parameters, the model output can be decomposed by different effects as shown:

$$f(X) = f_0 + \sum_{i}^{M} f_i(x_i) + \sum_{1<=i<=j<=M} f_{ij}(x_i, x_j) + ... + f_{1,2,...,M}(x_1, x_2, ..., x_M) \quad (3.37)$$

Consider only the constant term, first-order term and second-order term (which is sufficient for this case), the Equation (3.37) can be rewritten as:

$$f(X) = f_0 + \sum_{i}^{M} f_i(x_i) + \sum_{1<=i<=j<=M} f_{ij}(x_i, x_j) \quad (3.38)$$

Assume $f(x)$ is square integrable, and after squaring Equation (3.38) and integrating over the input space, the following equation can be obtained:

$$\int f^2(X)dX - f_0^2 = \sum_{i=1}^{M} \int f_1^2(x_i) + \sum_{1<=i<=j<=M} \int f_{ij}^2(x_i, x_j) \tag{3.39}$$

The left-hand side of Equation (3.39) is called total variance:

$$V = \int f^2(X)dX - f_0^2 \tag{3.40}$$

and the right-hand side is called partial variance:

$$\begin{aligned} V_i &= \sum_{i=1}^{M} \int f_1^2(x_i) \\ V_i j &= \sum_{1<=i<=j<=M} \int f_{ij}^2(x_i, x_j) \end{aligned} \tag{3.41}$$

The ration between partial variance and total variance gives the global sensitivity index. The first order (main effect) and total-order sensitivity index for the i-th input variable x_i can be defined by:

$$\begin{aligned} S_i &= \frac{V_i}{V} \\ S_{Ti} &= 1 - \frac{V_{\sim i}}{V} \end{aligned} \tag{3.42}$$

where the notation $V_{\sim i}$ indicates all variances caused by its interactions, of any order, with any other input variables except V_i

The first-order and total-order sensitivity index are two important indicators in Sobol for variable importance. In principle, the higher the index value, the more important the variable is, and vice versa. What this study interests in are the M independent parameters, therefore, with the assumption of inputs being independently and uniformly distributed within a unit hypercube, the value of sensitivity index computed is equlibrium to the relative importance of the parameters. Normally, for optimization purpose, those important parameters should be selected. However, the parameters here are hydrodynamic coefficients provided from the regression estimation with uncertain accuracy, and the least important ones are more likely to be those with deficiency, hence need to be optimized. Consequently, 5 hydrodynamic coefficients with lowest sensitivity indices from each degree of freedom are selected and grouped, which later form the target genes in

genetic algorithm. The diagram containing the details of the process of sensitivity analysis is displayed in figure 3.6.

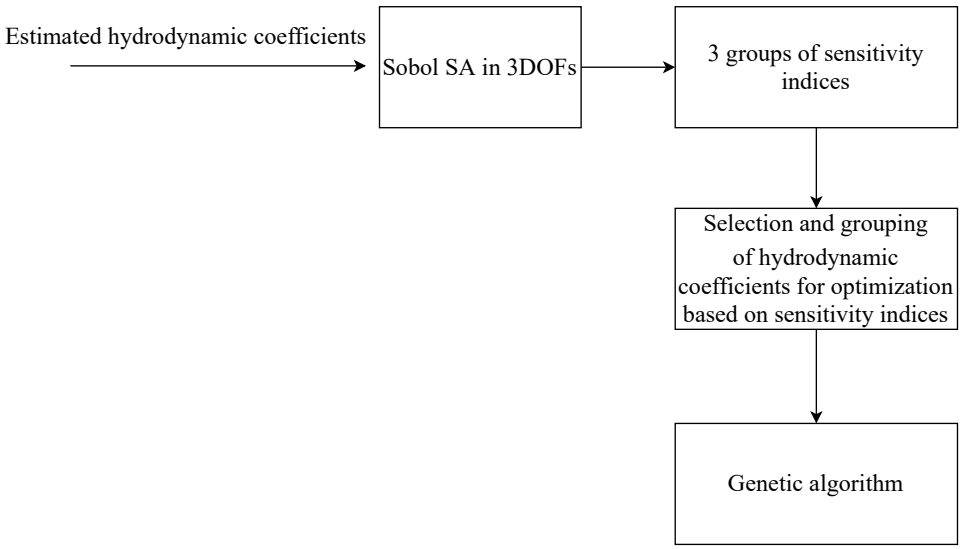

Figure 3.6: Diagram of SA

3.2.4 Optimization Method: Genetic Algorithm

As one of the most popular types of evolutionary algorithm (EA), genetic algorithm is widely employed for global optimization problems. It's also a derivative-free optimization method which is capable of providing high-quality solutions. However, it's a random-based approach where the changes are randomly given to the current solutions to generate new ones, which requires considerable computational time in order to obtain the best outcome.

Under the environmental effects of wind, the hydrodynamic coefficients identified by LS or SVM method might be corrupted to some extent, in which case, GA can be applied for improving the identified coefficients from the perspective of ship behaviours in global sense instead of learning algorithm based on data.

The general structure of GA consists of initialization, selection, crossover, mutation, termination. In this case, a set of hydrodynamic coefficients in total 40 is referred as one solution where each individual is called chromosome. It's noteworthy here, that only one full set of identified hydrodynamic coefficients is loaded into GA and 4 more identical solutions are added into the mating pool to enable GA to run properly. The mean squared error (MSE) method [Sun and Wang, 2012] is used to define the fitness function as shown in Equation (3.43) and the optimization process is presented in figure 3.7.

$$Fitness = \sum_{k}^{u,v,r} \frac{1}{N} \sum_{i=1}^{N} (k - \hat{k})^2 \tag{3.43}$$

Where $\hat{k}$ is the reference velocity component with respect to the estimated one k

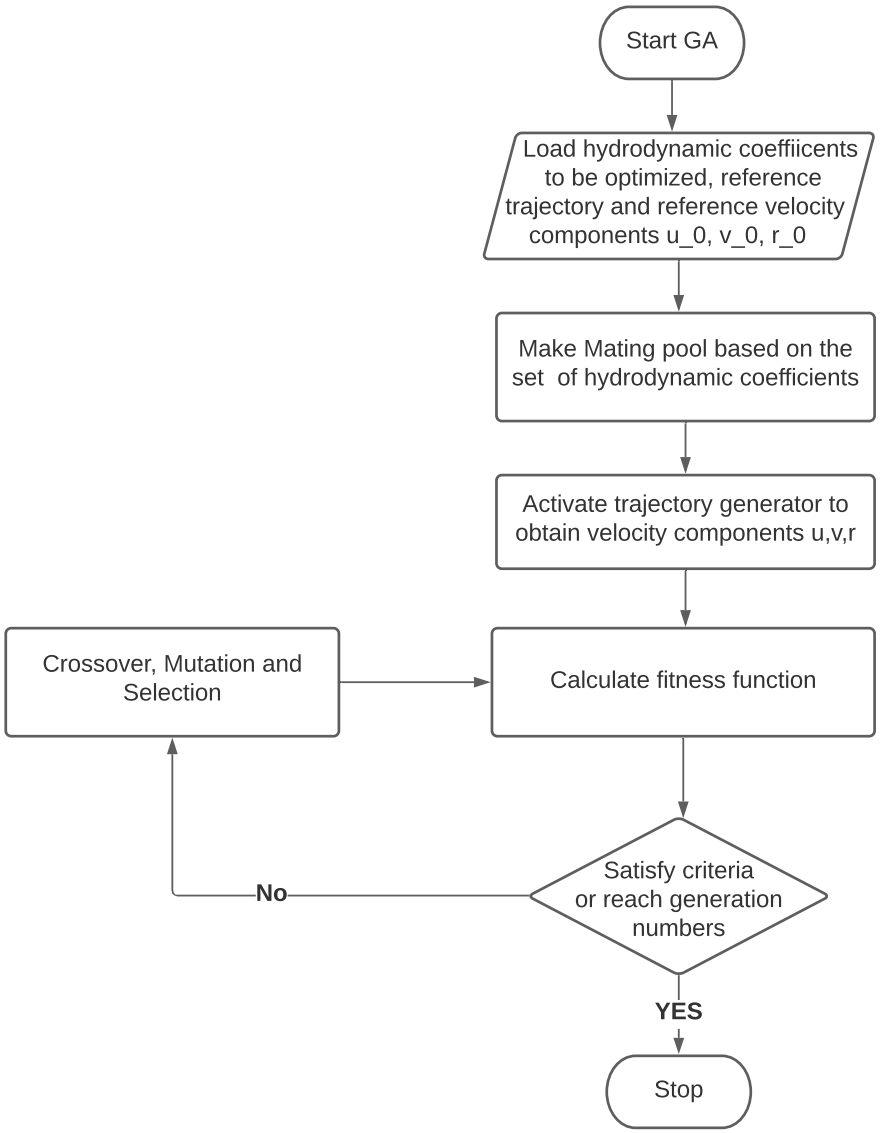

Figure 3.7: Structure of optimization process

Chapter 4

Experiments and Results

There are three sections in this chapter. Section one introduce the basic setup of experiment including simulation platforms, data, settings of Sobol and GA, noise generation and manoeuvring simulation. In section two, three groups of experiments are designed and conducted to identify hydrodynamic coefficients under different conditions. In addition, analyses are performed to study the effects of three important factors on the results of identification including wind speed, noise and wind direction. Last section carries out validation on LS+GA and SVM+GA in three extreme cases by means of trajectory and velocity comparison.

4.1 Experiment Setup

As discussed in the previous section, a mariner class cargo vessel is used as the research object. Principle parameters are listed in the table 4.1 below. As for wind force and moment calculation, considering it's hard to find the original ones, the ship parameters related are taken from similar vessel provided in [Fujiwara and Nimura, 2005], which are also given in the table 4.1.

The experiments are performed in Marine Systems Simulator (MSS) [Fossen and Perez, 2004], which is a Matlab and Simulink library for marine systems developed by Fossen and his associate. It contains toolbox for real-time simulation with various acknowledged vessel models available such as Mariner class vessel. Training data is generated using the MSS toolbox, and simple data processing is needed before parameter identification. Besides, zigzag manoeuvre of $20°/20°$is performed for data generation with time step of 0.1s, and the training data has a total number of 40001 data samples.

Sobol is employed in this study to select and group the hydrodynamic coefficients. The range of input variables is set as [0,1], and the sample number is taken as 5000. Besides, the sensitivity analysis model adopts Equation (3.5) and indices

of constant terms such as Y_0 and N_0 are regarded as 0 in SA. In the following experiments, S_1 is used as the main criterion for ranking given the fact that the SA model equations are linear and S_1 and S_T have close values as shown in table 4.2, and 5 coefficients with the lowest values are selected from each motion separately, which forms the 15 hydrodynamic coefficients to be optimized.

A genetic algorithm package developed by [Gad, 2021] is implemented for optimization purpose and with the great help of the author, it has been modified to fulfill the requirements of this study. 200 generations are run in the GA experiment and the crossover probability and mutation probability are set as 0.6 and 1, respectively. In addition, there are in total 40 genes for GA while 15 of them are subject to evolution, which corresponds to the 15 hydrodynamic coefficients to be optimized, and the lower bound and upper bound for each individual gene are defined respectively as 0.5 and 1.5 or 1.5 and 0.5 of itself depending on the positive or negative sign of the coefficient value. Last but not least, the stoping criteria is given as 1e-5 for all the cases.

Ship Parameters	Description
L	160.93 m
U_0	7.7175 m/s (15 knots)
m'	798e-5
I'_z	39.2e-5
x'_G	-0.023
$X'_{\dot{u}}$	-42e-5
$Y'_{\dot{v}}$	-748e-5
$Y'_{\dot{r}}$	-9.354e-5
$N'_{\dot{v}}$	4.64e-5
$N'_{\dot{r}}$	-43.8e-5
A_{Fw}	469 m^2
A_{Lw}	1874 m^2
S_L	7.2 m

Table 4.1: Ship parameters

Input variables	S_1	S_T	Hydrodynamic coefficients
r^2	0.000446	0.000436	X'_{rr}
$v * d$	0.005828	0.005985	X'_{vd}
u^2	0.005917	0.005978	X'_{uu}
$u * v * d$	0.006008	0.006001	X'_{uvd}
d^2	0.006374	0.006379	X'_{dd}
u	0.020702	0.02065	X'_{u}
u^3	0.022772	0.023317	X'_{uuu}
$u * d^2$	0.028243	0.027781	X'_{udd}
v^2	0.441506	0.439713	X'_{vv}
$r * v$	0.464346	0.462292	X'_{rv}

Table 4.2: An example of Sobol sensitivity analysis in surge motion

4.1.1 Noise Generation

The measurement noise of wind speed is considered in this paper, hence the experiments. The wind speed and its direction can be measured by an anemometer and a weathervane, respectively. For those anemometers that measure the wind speed, an accuracy is often used. The anemometer accuracy varies from device to device and sensor to sensor, therefore, it's more reasonable to study a range of accuracy instead of randomly assigning a number. Consequently, the range of accuracy is defined from -10% to + 10%, with an interval of 5%, and the actual wind speed is polluted with the defined accuracy which is shown as:

$$V_p = V_w(1 + accuracy) \tag{4.1}$$

4.1.2 Manoeuvring Simulation

There are two common ways to validate the results of parameter identification, one is by comparison between identified hydrodynamic coefficients and benchmarks obtained from PMM test, the other one is by testing generalization performance of the identified model, for which various manoeuvring simulations are carried out. In evaluation of generalization performance of the identified model, more manoeuvres are needed, which include zigzag test of 10°/10°and 40°/40°. In addition, the simulation is set as 600s with 0.1s time step and environmental condition is considered.

4.2 Identification Results

Table 4.3-4.5 present the comparisons of estimation results under calm water condition with the benchmarks [Chislett and Strom-Tejsen, 1965] in 3DOF. 20-20 zigzag manoeuvre is used to generate data in this case. With clean data set, almost all the hydrodynamic coefficients can be accurately estimated using either LS or SVM method. However, there are some small differences found in the results of SVM method such as Y'_{0uu} and N'_{0uu}, which may be due to the instability of the method or selection of regularization factor C.

	Original	LS	SVM
X'_u	-1.84E-03	-1.84E-03	-1.84E-03
X'_{uu}	-1.10E-03	-1.10E-03	-1.09E-03
X'_{uuu}	-2.15E-03	-2.15E-03	-2.12E-03
X'_{vv}	-8.99E-03	-8.99E-03	-8.99E-03
X'_{rr}	1.80E-04	1.80E-04	1.80E-04
X'_{rv}	7.98E-03	7.98E-03	7.98E-03
X'_{dd}	-9.50E-04	-9.50E-04	-9.50E-04
X'_{udd}	-1.90E-03	-1.90E-03	-1.90E-03
X'_{vd}	9.30E-04	9.30E-04	9.30E-04
X'_{uvd}	9.30E-04	9.30E-04	9.30E-04

Table 4.3: Comparison of identified hydrodynamic coefficients in surge motion with clean data

	Original	LS	SVM
Y'_v	-1.16E-02	-1.16E-02	-1.16E-02
Y'_r	-4.99E-03	-4.99E-03	-4.98E-03
Y'_{vvv}	-8.08E-02	-8.08E-02	-8.23E-02
Y'_{vvr}	1.54E-01	1.54E-01	1.53E-01
Y'_{vu}	-1.16E-02	-1.16E-02	-1.17E-02
Y'_{ru}	-4.99E-03	-4.99E-03	-5.05E-03
Y'_d	2.78E-03	2.78E-03	2.78E-03
Y'_{ddd}	-9.00E-04	-9.00E-04	-9.03E-04
Y'_{ud}	5.56E-03	5.56E-03	5.53E-03
Y'_{uud}	2.78E-03	2.78E-03	2.71E-03
Y'_{vdd}	-4.00E-05	-4.00E-05	-2.94E-05
Y'_{vvd}	1.19E-02	1.19E-02	1.15E-02
Y'_0	-4.00E-05	-4.00E-05	-3.97E-05
Y'_{0u}	-8.00E-05	-8.00E-05	-7.54E-05
Y'_{0uu}	-4.00E-05	-4.00E-05	-1.75E-05

Table 4.4: Comparison of identified hydrodynamic coefficients in sway motion with clean data

	Original	LS	SVM
N'_v	- 2.64E-03	-2.64E-03	-2.65E-03
N'_r	-1.66E-03	-1.66E-03	-1.67E-03
N'_{vvv}	1.64E-02	1.64E-02	1.82E-02
N'_{vvr}	-5.48E-02	-5.48E-02	-5.37E-02
N'_{vu}	-2.64E-03	-2.64E-03	-2.50E-03
N'_{ru}	-1.66E-03	-1.66E-03	-1.59E-03
N'_d	-1.39E-03	-1.39E-03	-1.39E-03
N'_{ddd}	4.50E-04	4.50E-04	4.53E-04
N'_{ud}	-2.78E-03	-2.78E-03	-2.74E-03
N'_{uud}	-1.39E-03	-1.39E-03	-1.31E-03
N'_{vdd}	1.30E-04	1.30E-04	1.17E-04
N'_{vvd}	-4.89E-03	-4.89E-03	-4.36E-03
N'_0	3.00E-05	3.00E-05	2.99E-05
N'_{0u}	6.00E-05	6.00E-05	5.44E-05
N'_{0uu}	3.00E-05	3.00E-05	2.62E-06

Table 4.5: Comparison of identified hydrodynamic coefficients in yaw motion with clean data

4.2.1 Wind Speed

To begin with, -5% noise level and 45°wind direction are kept the same in the first group of experiments on the effect of wind speed. Table 4.6-4.8 provide comparisons of identification results in four wind speeds, 4m/s, 8m/s, 12m/s and 16m/s. A quantitative factor $deviation = \frac{identified\ result - benchmark}{benchmark} \times 100\%$ is defined for better visualization of the identification accuracy. Apart from that, those selected hydrodynamic coefficients for optimization are highlighted in the columns of LS+GA and SVM+GA in the table.

As can be seen from the tables, most of the hydrodynamic coefficients estimated by LS or SVM method show good agreement with benchmarks in all cases while some of them have rather high deviations including X'_{rr}, Y'_{vdd}, Y'_{0uu} and N'_{0uu}. Moreover, the accuracy of X'_{rr} and X'_{rrr} seems to increase with higher wind speed in LS results, and similar pattern is found in SVM results from 4m/s to 12m/s except for the case of 16m/s where deviations are as high as 32.59% and 47.54% respectively.

As for the other two methods, despite of small improvement in X'_{uuu} and X'_{rr}, deviations of other coefficients after optimization even increase in the case of 4m/s and 8m/s in LS+GA method, whereas the results of SVM+GA stay unchanged after optimization due to the low fitness value close to stoping criteria. In the case of 12m/s, coefficients X'_{rr}, Y'_0, Y'_{0u}, Y'_{0uu} as well as N'_0, N'_{0u}, N'_{0uu} are evolved into better results in LS+GA method and coefficients Y'_{vdd}, Y'_0, Y'_{0u} and Y'_{0uu} are effectively optimized in SVM+GA method. Besides, in the case of 16m/s, deviations of X'_{uvd} Y'_{0uu}, N'_{0u} and N'_{0uu} are slightly reduced with optimization in LS+GA method, and results of X'_{uu}, Y'_{0uu}, N'_{vdd}, N'_{0u} along with N'_{0uu} also become better in SVM+GA method.

To better analysis the results, system performance comparison is conducted on zig-zag manoeuvres 10°/10°, 20°/20°and 40°/40°using fitness function defined in Equation(3.43). The fitness value indicates the velocities difference between trajectory generated using identified model and reference trajectory generated with original model, and the larger the value, the poorer performance it has. The identification wind speed corresponds to the model identified under such wind speed. Additionally, all the cases are simulated under wind condition with speed of 10m/s and direction of 45°.

From the comparison curves provided in figure 4.1, one can easily find SVM has best performance in the case of 4m/s, 8m/s and 12m/s in three simulated manoeuvres while in the case of 16m/s in zigzag 20°/20°, SVM+GA outperforms it with small margin. What's more, models identified by LS+GA under 12 m/s and 16 m/s wind have better performance in zigzag10°/10°and zigzag 20°/20°respectively compared to those by LS. Apart from that, one can also notice LS+GA and SVM+GA have the worst outcome in the case of 12m/s and 16m/s in zigzag 40°/40°.

	Deviation(%) (4m/s)				Deviation(%) (8m/s)			
	LS	LS+GA	SVM	SVM+GA	LS	LS+GA	SVM	SVM+GA
X'_u	-1.86	-1.86	-1.36	-1.36	-2.59	-2.59	-1.05	-1.05
X'_{uu}	-34.91	-60.85	-30.40	-30.40	-32.89	-28.27	-18.89	-18.89
X'_{uuu}	-63.67	-63.27	-57.07	-57.07	-54.08	-40.98	-34.66	-34.66
X'_{vv}	-3.76	-3.76	-3.77	-3.77	-7.19	-7.19	-7.17	-7.17
X'_{rr}	20.35	10.09	20.53	20.53	39.66	36.47	39.81	39.81
X'_{rv}	2.65	2.65	2.67	2.67	5.22	5.22	5.21	5.21
X'_{dd}	0.98	3.87	0.27	0.27	2.74	9.79	0.75	0.75
X'_{udd}	1.73	1.73	-0.26	-0.26	5.40	5.40	0.11	0.11
X'_{vd}	1.48	11.61	1.38	1.38	3.14	-46.37	2.84	2.84
X'_{uvd}	3.97	3.97	3.50	3.50	6.01	6.01	4.67	4.67
	Deviation(%) (12m/s)				Deviation(%) (16m/s)			
	LS	LS+GA	SVM	SVM+GA	LS	LS+GA	SVM	SVM+GA
X'_u	-2.75	-2.75	0.24	0.24	-3.64	-3.64	1.03	1.03
X'_{uu}	-12.49	-51.61	12.90	-11.98	-4.39	40.84	32.59	24.84
X'_{uuu}	-11.57	-11.57	19.80	19.80	8.36	8.36	47.54	47.54
X'_{vv}	-8.20	-8.20	-8.13	-8.13	-7.43	-7.43	-7.42	-7.42
X'_{rr}	44.90	-26.52	45.49	88.61	37.47	54.96	37.88	89.91
X'_{rv}	6.09	6.09	6.03	6.03	5.57	5.57	5.50	5.50
X'_{dd}	4.72	10.10	1.04	8.17	6.50	-26.26	0.93	16.32
X'_{udd}	9.27	9.27	0.06	0.06	11.81	11.81	-0.72	-0.72
X'_{vd}	3.38	-28.80	2.65	-26.15	2.81	-44.27	1.38	33.91
X'_{uvd}	3.77	-20.29	0.89	16.20	3.49	1.81	-1.88	11.62

Table 4.6: Comparison of identified hydrodynamic coefficients in surge motion in different wind speeds

	Deviation(%) (4m/s)				Deviation(%) (8m/s)			
	LS	LS+GA	SVM	SVM+GA	LS	LS+GA	SVM	SVM+GA
Y'_{v}	0.21	0.21	0.18	0.18	0.31	0.31	0.29	0.29
Y'_{r}	0.32	0.32	0.28	0.28	0.47	0.47	0.44	0.44
Y'_{vvv}	-3.25	-3.25	-3.08	-3.08	-4.08	-4.08	-4.06	-4.06
Y'_{vvr}	0.88	0.88	0.83	0.83	0.63	0.63	0.64	0.64
Y'_{vu}	0.23	0.23	0.22	0.22	3.53	3.53	3.36	3.36
Y'_{ru}	0.16	0.16	0.18	0.18	3.63	3.63	3.46	3.46
Y'_{d}	-0.24	-0.24	-0.22	-0.22	-0.28	-0.28	-0.26	-0.26
Y'_{ddd}	-0.44	-15.31	-0.42	-0.42	-0.15	5.80	-0.16	-0.16
Y'_{ud}	1.39	1.39	1.39	1.39	3.08	3.08	3.23	3.23
Y'_{uud}	13.41	13.41	13.47	13.47	33.21	33.21	34.10	34.10
Y'_{vdd}	74.06	75.78	72.43	72.43	129.40	198.28	127.97	127.97
Y'_{vvd}	5.75	5.75	5.34	5.34	5.23	5.23	5.28	5.28
Y'_{0}	-4.95	29.36	-5.07	-5.07	-18.51	-47.68	-19.29	-19.29
Y'_{0u}	28.35	75.76	26.26	26.26	41.64	15.04	38.74	38.74
Y'_{0uu}	240.42	354.62	224.90	224.90	326.28	130.66	304.27	304.27
	Deviation(%) (12m/s)				Deviation(%) (16m/s)			
	LS	LS+GA	SVM	SVM+GA	LS	LS+GA	SVM	SVM+GA
Y'_{v}	-0.06	-0.06	-0.09	-0.09	-0.76	-0.76	-0.76	-0.76
Y'_{r}	0.08	0.08	0.07	0.07	-0.55	-0.55	-0.56	-0.56
Y'_{vvv}	-1.61	-1.61	-1.59	-1.59	4.27	4.27	4.29	4.29
Y'_{vvr}	-1.01	-1.01	-1.00	-1.00	-3.76	-3.76	-3.75	-3.75
Y'_{vu}	7.29	7.29	7.07	7.07	11.15	11.15	11.08	11.08
Y'_{ru}	7.83	7.83	7.60	7.60	11.98	11.98	11.84	11.84
Y'_{d}	0.03	0.03	0.06	0.06	0.58	0.58	0.59	0.59
Y'_{ddd}	0.27	-46.35	0.28	-18.13	-0.16	-42.37	-0.07	20.01
Y'_{ud}	4.35	4.35	4.52	4.52	5.62	5.62	5.60	5.60
Y'_{uud}	46.18	46.18	47.01	47.01	53.99	53.99	53.80	53.80
Y'_{vdd}	135.91	249.41	134.65	25.21	80.75	140.50	77.93	95.59
Y'_{vvd}	-2.23	-2.23	-2.02	-2.02	-12.91	-12.91	-12.70	-12.70
Y'_{0}	-40.71	-40.63	-43.60	-33.08	-74.79	-78.35	-78.25	-81.62
Y'_{0u}	9.05	1.17	6.05	1.94	-124.67	-127.28	-126.32	-130.54
Y'_{0uu}	117.48	106.48	83.30	61.93	-646.32	-618.98	-657.54	-558.04

Table 4.7: Comparison of identified hydrodynamic coefficients in sway motion in different wind speeds

	Deviation(%) (4m/s)				Deviation(%) (8m/s)			
	LS	LS+GA	SVM	SVM+GA	LS	LS+GA	SVM	SVM+GA
N'_v	0.26	0.26	0.26	0.26	0.60	0.60	0.54	0.54
N'_r	0.29	0.29	0.31	0.31	0.63	0.63	0.59	0.59
N'_{vvv}	5.81	5.81	6.29	6.29	10.18	10.18	10.14	10.14
N'_{vvr}	-1.00	-1.00	-1.09	-1.09	-1.70	-1.70	-1.70	-1.70
N'_{vu}	-1.29	-1.29	-1.60	-1.60	-1.36	-1.36	-1.65	-1.65
N'_{ru}	-1.03	-1.03	-1.25	-1.25	-1.13	-1.13	-1.30	-1.30
N'_d	0.17	0.17	0.18	0.18	0.38	0.38	0.36	0.36
N'_{ddd}	0.41	16.50	0.42	0.42	0.59	-45.65	0.59	0.59
N'_{ud}	-0.76	-0.76	-0.88	-0.88	-1.56	-1.56	-1.69	-1.69
N'_{uud}	-5.99	-5.99	-6.69	-6.69	-13.60	-13.60	-14.47	-14.47
N'_{vdd}	-6.84	5.30	-7.08	-7.08	-9.38	-42.42	-9.24	-9.24
N'_{vvd}	-5.61	-5.61	-6.06	-6.06	-10.60	-10.60	-10.52	-10.52
N'_0	1.55	-28.43	1.60	1.60	4.74	-4.70	4.93	4.93
N'_{0u}	-11.75	-21.41	-11.75	-11.75	-31.37	-57.82	-29.55	-29.55
N'_{0uu}	-101.06	-100.82	-100.67	-100.67	-256.08	-269.99	-242.77	-242.77
	Deviation(%) (12m/s)				Deviation(%) (16m/s)			
	LS	LS+GA	SVM	SVM+GA	LS	LS+GA	SVM	SVM+GA
N'_v	0.37	0.37	0.26	0.26	-0.65	-0.65	-0.80	-0.80
N'_r	0.47	0.47	0.41	0.41	-0.46	-0.46	-0.50	-0.50
N'_{vvv}	10.25	10.25	10.20	10.20	5.20	5.20	5.14	5.14
N'_{vvr}	-1.46	-1.46	-1.48	-1.48	-0.11	-0.11	-0.13	-0.13
N'_{vu}	-1.83	-1.83	-2.43	-2.43	-4.42	-4.42	-5.16	-5.16
N'_{ru}	-1.34	-1.34	-1.66	-1.66	-3.33	-3.33	-3.68	-3.68
N'_d	0.46	0.46	0.42	0.42	0.26	0.26	0.18	0.18
N'_{ddd}	0.58	-16.63	0.59	-14.02	0.77	8.53	0.89	-4.52
N'_{ud}	-1.58	-1.58	-1.85	-1.85	-1.65	-1.65	-1.96	-1.96
N'_{uud}	-13.15	-13.15	-14.73	-14.73	-8.40	-8.40	-10.02	-10.02
N'_{vdd}	-4.92	17.70	-4.75	27.73	16.98	50.72	17.00	8.21
N'_{vvd}	-11.95	-11.95	-11.98	-11.98	-11.10	-11.10	-11.08	-11.08
N'_0	9.02	-2.44	10.28	18.91	14.63	-12.66	16.39	-33.52
N'_{0u}	-51.52	-42.46	-47.93	-62.84	-46.65	-40.16	-40.69	-37.02
N'_{0uu}	-380.71	-324.11	-351.23	-406.44	-257.51	-234.22	-214.78	-179.40

Table 4.8: Comparison of identified hydrodynamic coefficients in yaw motion in different wind speeds

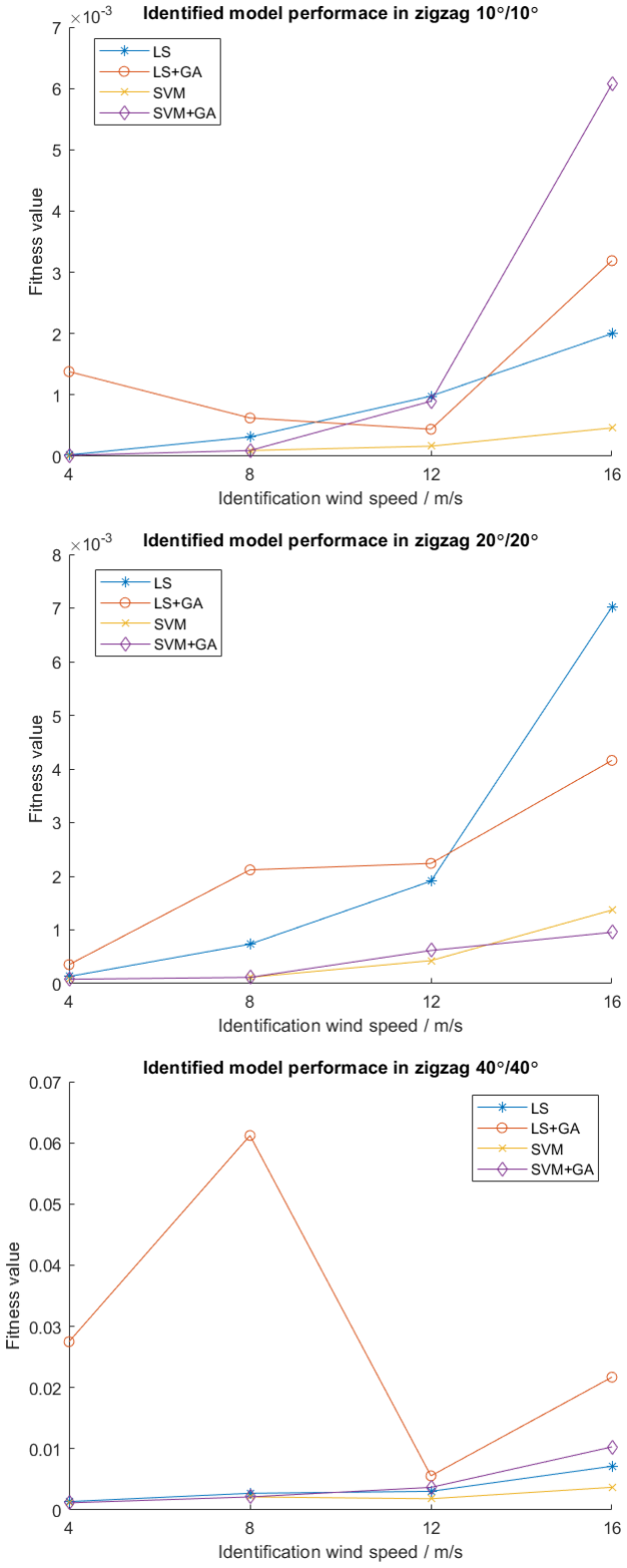

Figure 4.1: System performance comparison one

4.2.2 Noise in Wind Speed

Then, the following experiments aim to analysis the effect of measurement noise in wind speed on the results of identification, and considering that Beaufort scale 6 might be more frequently encountered in practice, wind speed of 12m/s in direction of 45°is adopted as the environmental condition. 4 noise levels -5%, -10%, 5% and 10% are studied, and the comparisons are shown in the table 4.9-4.11.

For many of the hydrodynamic coefficients, both LS and SVM method are able to estimate the values with a relative low deviation in four noise levels, but the results of -10% noise and 10% noise are worse compared to those of -5% and 5%. What's more, it seems the deviation follows a linear relationship with respect to noise level, for instance, deviations of X'_{rr} at noise level -10%, -5%, 5% and 10% are 87.79%, 44.9%, -46.91% and -95.83%, respectively. In additional, coefficient X'_{uu}, X'_{uuu}, X'_{rr}, Y'_{udd}, Y'_{vdd}, Y'_{0}, Y'_{0uu}, N'_{0u} and N'_{0uu} suffer more negative effect from noise compared with others.

In the case of -5% noise, only deviations of coefficient Y'_{0}, Y'_{0u} and Y'_{0uu} are reduced in SVM+GA, and in LS+GA, three more are lowered, which are N'_{0}, N'_{0u} and N'_{0uu}. While in the case of 5% noise, all the selected coefficients in sway motion are optimized along with X'_{rr}, N'_{0} and N'_{0uu} in LS+GA, and in SVM+GA, results of X'_{rr}, Y'_{udd} and N'_{0uu} are slightly improved. Furthermore, there are 5 selected coefficients which are effectively optimized in LS+GA in the case of -10% noise, including X'_{uu}, X'_{dd}, Y'_{vdd}, Y'_{0u}, Y'_{0uu}, and same amounts are found in SVM+GA which are Y'_{vdd}, Y'_{0u}, Y'_{0uu}, N'_{vdd} and N'_{0}. Last but not least, in the case of 10%, coefficient Y'_{vdd}, Y'_{0}, Y'_{0u}, N'_{0} as well as N'_{0u} have slightly better results in LS+GA and SVM+GA compared with those of LS and SVM accordingly.

A similar approach as Section 4.2.1 can be applied to analysis the system performance of identified models in zigzag manoeuvres and the comparison curves are shown in figure 4.2. Identification noise corresponds to the set of hydrodynamic coefficients identified at such noise level. As can be seen from the figure, SVM+GA has the best performance in the case of 10% noise in zigzag 20°/20°and 40°/40°, and generalization performance of SVM is the best when looking through all 3 comparisons. Moreover, LS+GA is better at noise level of -5% and 10% compared to that of LS in the case of zigzag 10°/10°while In the case of 20°/20°, higher performance of LS+GA is found at 5% and 10% noise compared to that of LS.

	Deviation(%) (-5%)				Deviation(%) (-10%)			
	LS	LS+GA	SVM	SVM+GA	LS	LS+GA	SVM	SVM+GA
X'_u	-2.75	-2.75	0.24	0.24	-5.44	-5.44	0.42	0.42
X'_{uu}	-12.49	-51.61	12.90	-11.98	-25.31	-5.79	24.67	64.61
X'_{uuu}	-11.57	-11.57	19.80	19.80	-23.97	-23.97	37.73	37.73
X'_{vv}	-8.20	-8.20	-8.13	-8.13	-16.06	-16.06	-15.91	-15.91
X'_{rr}	44.90	-26.52	45.49	88.61	87.79	142.95	88.45	90.53
X'_{rv}	6.09	6.09	6.03	6.03	11.92	11.92	11.80	11.80
X'_{dd}	4.72	10.10	1.04	8.17	9.27	-7.33	1.85	-24.20
X'_{udd}	9.27	9.27	0.06	0.06	18.23	18.23	0.17	0.17
X'_{vd}	3.38	-28.80	2.65	-26.15	6.68	50.71	5.32	-20.02
X'_{uvd}	3.77	-20.29	0.89	16.20	7.66	-19.43	1.96	-18.83
	Deviation(%) (5%)				Deviation(%) (10%)			
	LS	LS+GA	SVM	SVM+GA	LS	LS+GA	SVM	SVM+GA
X'_u	2.81	2.81	-0.26	-0.26	5.67	5.67	-0.58	-0.58
X'_{uu}	12.17	47.39	-14.10	-17.41	24.04	36.94	-29.25	-25.52
X'_{uuu}	10.76	10.76	-21.61	-21.61	20.74	20.74	-45.01	-45.01
X'_{vv}	8.54	8.54	8.47	8.47	17.43	17.43	17.28	17.28
X'_{rr}	-46.91	-36.36	-46.96	-39.35	-95.83	-96.22	-96.37	-97.02
X'_{rv}	-6.35	-6.35	-6.30	-6.30	-12.97	-12.97	-12.84	-12.84
X'_{dd}	-4.88	-8.37	-1.02	17.07	-9.93	1.46	-2.11	-21.65
X'_{udd}	-9.57	-9.57	-0.07	-0.07	-19.45	-19.45	-0.20	-0.20
X'_{vd}	-3.45	-50.21	-2.69	34.79	-6.98	-20.72	-5.50	-48.55
X'_{uvd}	-3.63	37.15	-0.66	-49.06	-7.11	19.43	-1.07	-43.19

Table 4.9: Comparison of identified hydrodynamic coefficients in surge motion at different noise levels

	Deviation(%) (-5%)				Deviation(%) (-10%)			
	LS	LS+GA	SVM	SVM+GA	LS	LS+GA	SVM	SVM+GA
Y'_{v}	-0.06	-0.06	-0.09	-0.09	-0.13	-0.13	-0.18	-0.18
Y'_{r}	0.08	0.08	0.07	0.07	0.15	0.15	0.12	0.12
Y'_{vvv}	-1.61	-1.61	-1.59	-1.59	-3.04	-3.04	-2.99	-2.99
Y'_{vvr}	-1.01	-1.01	-1.00	-1.00	-2.01	-2.01	-1.98	-1.98
Y'_{vu}	7.29	7.29	7.07	7.07	14.30	14.30	13.88	13.88
Y'_{ru}	7.83	7.83	7.60	7.60	15.38	15.38	14.93	14.93
Y'_{d}	0.03	0.03	0.06	0.06	0.07	0.07	0.10	0.10
Y'_{ddd}	0.27	-46.35	0.28	-18.13	0.57	-28.76	0.58	-30.13
Y'_{ud}	4.35	4.35	4.52	4.52	8.50	8.50	8.81	8.81
Y'_{uud}	46.18	46.18	47.01	47.01	90.37	90.37	91.97	91.97
Y'_{vdd}	135.91	249.41	134.65	25.21	268.53	156.04	267.10	85.90
Y'_{vvd}	-2.23	-2.23	-2.02	-2.02	-4.60	-4.60	-4.20	-4.20
Y'_{0}	-40.71	-40.63	-43.60	-33.08	-79.81	-85.72	-83.09	-83.62
Y'_{0u}	9.05	1.17	6.05	1.94	16.14	7.57	8.63	-2.64
Y'_{0uu}	117.48	106.48	83.30	61.93	218.36	66.95	153.23	82.95
	Deviation(%) (5%)				Deviation(%) (10%)			
	LS	LS+GA	SVM	SVM+GA	LS	LS+GA	SVM	SVM+GA
Y'_{v}	0.06	0.06	0.09	0.09	0.11	0.11	0.17	0.17
Y'_{r}	-0.09	-0.09	-0.08	-0.08	-0.20	-0.20	-0.16	-0.16
Y'_{vvv}	1.80	1.80	1.77	1.77	3.78	3.78	3.72	3.72
Y'_{vvr}	1.03	1.03	1.02	1.02	2.07	2.07	2.05	2.05
Y'_{vu}	-7.56	-7.56	-7.32	-7.32	-15.38	-15.38	-14.89	-14.89
Y'_{ru}	-8.11	-8.11	-7.87	-7.87	-16.50	-16.50	-16.01	-16.01
Y'_{d}	-0.02	-0.02	-0.03	-0.03	-0.03	-0.03	-0.02	-0.02
Y'_{ddd}	-0.24	-0.24	-0.30	-0.30	-0.45	-0.45	-0.57	-0.57
Y'_{ud}	-4.54	-4.54	-4.72	-4.72	-9.26	-9.26	-9.63	-9.63
Y'_{uud}	-48.14	-30.49	-49.04	-56.74	-98.20	-97.59	-100.06	-100.07
Y'_{vdd}	-139.25	-134.68	-137.35	-135.23	-281.79	-280.28	-277.75	-266.32
Y'_{vvd}	2.08	2.08	1.87	1.87	4.01	4.01	3.58	3.58
Y'_{0}	42.31	-3.74	42.74	59.20	86.22	85.77	86.16	12.26
Y'_{0u}	-11.11	-27.20	-5.66	30.56	-24.32	12.32	-16.41	3.61
Y'_{0uu}	-134.71	-125.64	-99.86	-99.83	-286.87	-295.57	-215.08	-262.74

Table 4.10: Comparison of identified hydrodynamic coefficients in sway motion at different noise levels

	Deviation(%) (-5%)				Deviation(%) (-10%)			
	LS	LS+GA	SVM	SVM+GA	LS	LS+GA	SVM	SVM+GA
N'_v	0.37	0.37	0.26	0.26	0.72	0.72	0.51	0.51
N'_r	0.47	0.47	0.41	0.41	0.90	0.90	0.81	0.81
N'_{vvv}	10.25	10.25	10.20	10.20	19.89	19.89	19.79	19.79
N'_{vvr}	-1.46	-1.46	-1.48	-1.48	-2.83	-2.83	-2.85	-2.85
N'_{vu}	-1.83	-1.83	-2.43	-2.43	-3.42	-3.42	-4.58	-4.58
N'_{ru}	-1.34	-1.34	-1.66	-1.66	-2.49	-2.49	-3.13	-3.13
N'_d	0.46	0.46	0.42	0.42	0.89	0.89	0.84	0.84
N'_{ddd}	0.58	-16.63	0.59	-14.02	1.12	3.25	1.13	41.78
N'_{ud}	-1.58	-1.58	-1.85	-1.85	-3.10	-3.10	-3.62	-3.62
N'_{uud}	-13.15	-13.15	-14.73	-14.73	-25.93	-25.93	-28.98	-28.98
N'_{vdd}	-4.92	17.70	-4.75	27.73	-9.93	-24.17	-9.64	2.14
N'_{vvd}	-11.95	-11.95	-11.98	-11.98	-23.12	-23.12	-23.17	-23.17
N'_0	9.02	-2.44	10.28	18.91	17.82	46.72	19.66	-11.97
N'_{0u}	-51.52	-42.46	-47.93	-62.84	-99.53	-99.42	-90.95	-94.66
N'_{0uu}	-380.71	-324.11	-351.23	-406.44	-735.49	-924.13	-679.69	-855.96
	Deviation(%) (5%)				Deviation(%) (10%)			
	LS	LS+GA	SVM	SVM+GA	LS	LS+GA	SVM	SVM+GA
N'_v	-0.40	-0.40	-0.30	-0.30	-0.84	-0.84	-0.60	-0.60
N'_r	-0.50	-0.50	-0.43	-0.43	-1.02	-1.02	-0.91	-0.91
N'_{vvv}	-10.84	-10.84	-10.79	-10.79	-22.28	-22.28	-22.17	-22.17
N'_{vvr}	1.56	1.56	1.58	1.58	3.23	3.23	3.26	3.26
N'_{vu}	2.08	2.08	2.72	2.72	4.41	4.41	5.71	5.71
N'_{ru}	1.52	1.52	1.87	1.87	3.23	3.23	3.97	3.97
N'_d	-0.49	-0.49	-0.45	-0.45	-1.01	-1.01	-0.95	-0.95
N'_{ddd}	-0.62	-20.21	-0.68	-27.77	-1.27	-27.71	-1.36	44.88
N'_{ud}	1.63	1.63	1.92	1.92	3.30	3.30	3.88	3.88
N'_{uud}	13.50	13.50	15.19	15.19	27.33	27.33	30.84	30.84
N'_{vdd}	4.84	-46.89	4.53	-19.57	9.61	7.16	9.35	14.28
N'_{vvd}	12.73	12.73	12.76	12.76	26.25	26.25	26.31	26.31
N'_0	-9.24	-2.70	-9.21	14.64	-18.71	-1.60	-18.90	3.85
N'_{0u}	55.01	77.12	51.78	125.94	113.51	88.73	104.48	69.55
N'_{0uu}	406.51	395.56	374.64	370.46	838.68	1074.96	775.27	769.14

Table 4.11: Comparison of identified hydrodynamic coefficients in yaw motion at different noise levels

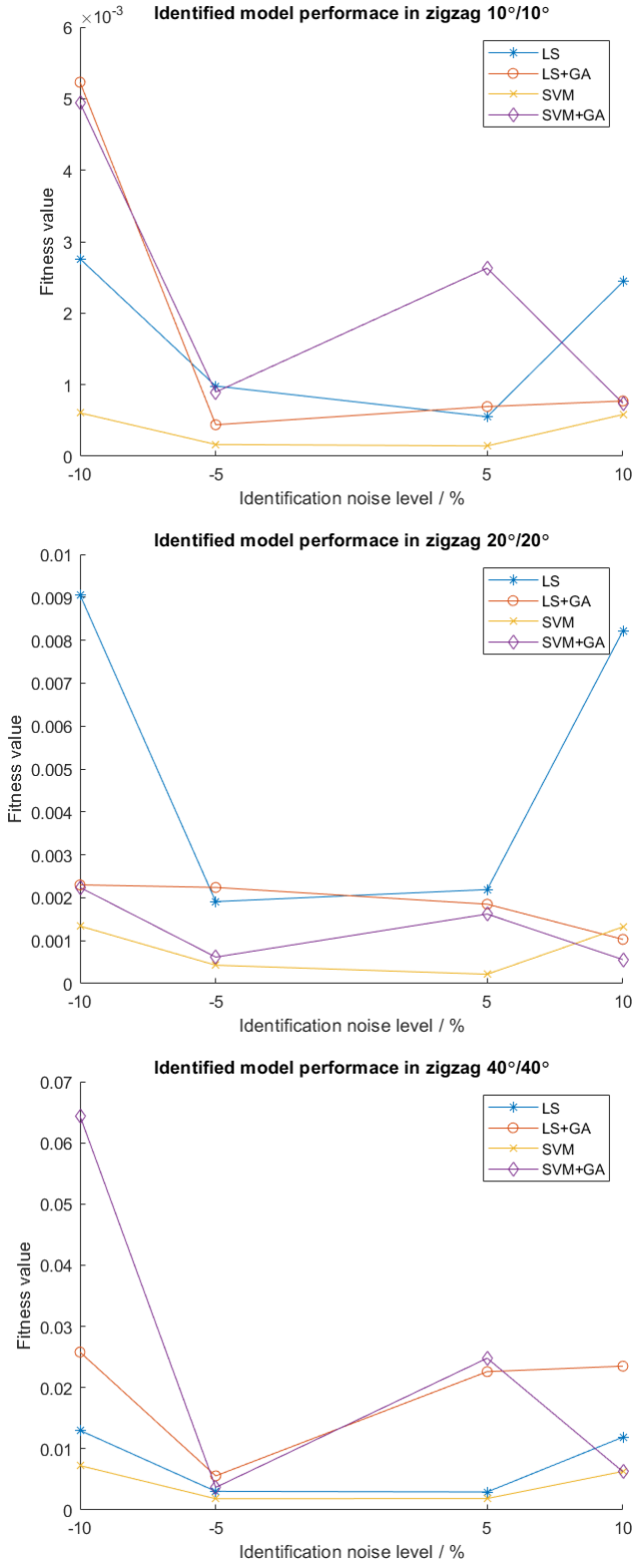

Figure 4.2: System performance comparison two

4.2.3 Wind Direction

The experiments succeeding are carried out to study the effect of different wind directions and the corresponding results are provided in table 4.12-4.14. The identification wind speed maintains at 12m/s with -5% noise and 4 directions -45°, -90°, 45°and 90°are investigated.

LS and SVM method have pretty similar identification results in four cases, where many deviations of direction -90°and 90°are higher than those of direction -45°and 45°, coefficient X'_{uu}, X'_{uuu}, X'_{rr}, Y'_{0u}, Y'_{0uu} in particular. Besides, results of direction -90°seems to be the worst among them with coefficients in all 3DOF severely deviated from their true values. Apart from that, deviations of X'_{rr}, Y'_{uud} and Y'_{vdd} are relatively high in all cases.

When it comes to the case of -45°, only coefficient X'_{rr}, Y'_0, Y'_{0uu} and N'_0 are improved in LS+GA along with coefficient Y'_0, N'_0 and N'_{0uu} in SVM+GA. As for case of 45°, the selected coefficients in surge motion are worse in LS+GA and SVM+GA compared to those of LS and GA respectively, but results of Y'_0, Y'_{0u}, Y'_{0uu}, N'_{0u} and N'_{0uu} in LS+GA are moderately improved as well as results of Y'_{vdd}, Y'_0, Y'_{0u} and Y'_{0uu} in SVM+GA. Additionally, in the case of 90°, deviations of coefficient X'_{rr}, Y'_{uud}, Y'_0 and N'_{0u} in LS+GA are lower compared to those of LS, and coefficient X'_{uvd}, Y'_{uud}, Y'_{vdd}, Y'_0, Y'_{0u}, Y'_{0uu}, N'_{vdd} have better accuracy compared to that of SVM. Lastly, in the case of -90°, optimization failed to improve the results of selected coefficients in surge motion and Y'_{0uu}, whose deviation is extremely high for both LS+GA and SVM+GA. Still, there are some coefficients optimized such as Y'_{uud}, Y'_0, N'_{vdd} and N'_0 in LS+GA and Y'_{uud}, Y'_0, Y'_{0u}, N'_0, N'_{0u} and N'_{0uu} in SVM+GA.

The system performance curves are presented in figure 4.3 for this study case with same environmental condition as the previous two. In zigzag 10°/10°, LS+GA and SVM+GA have best performance in the case of direction -45°and SVM+GA also has best performance in the case of direction -90°. Besides, performance of SVM+GA is the highest in the case of direction -45°and -90°in zigzag 20°/20°and LS+GA beats the rest in the case of direction 90°in same manoeuvre. Again, in zigzag 40°/40°, LS and SVM have prominent compared with other two.

	Deviation(%) (-45°)				Deviation(%) (-90°)			
	LS	LS+GA	SVM	SVM+GA	LS	LS+GA	SVM	SVM+GA
X'_u	-1.64	-1.64	1.10	1.10	1.01	4.50	1.69	-5.68
X'_{uu}	14.53	35.68	36.10	56.91	71.10	71.10	75.15	75.15
X'_{uuu}	33.27	33.27	58.53	58.53	148.05	148.05	152.67	152.67
X'_{vv}	-5.69	-5.69	-5.66	-5.66	-9.48	-9.48	-9.50	-9.50
X'_{rr}	29.51	-5.92	29.23	-31.26	67.43	130.27	67.81	95.12
X'_{rv}	4.09	4.09	4.05	4.05	7.92	7.92	7.92	7.92
X'_{dd}	3.80	-15.54	0.35	-11.93	1.21	13.47	0.12	-20.46
X'_{udd}	7.79	7.79	-0.94	-0.94	1.48	1.48	-1.43	-1.43
X'_{vd}	3.11	50.82	2.93	-3.31	2.83	52.38	2.69	40.85
X'_{uvd}	5.16	24.74	4.58	-25.78	-2.26	34.13	-2.63	11.80
	Deviation(%) (45°)				Deviation(%) (90°)			
	LS	LS+GA	SVM	SVM+GA	LS	LS+GA	SVM	SVM+GA
X'_u	-2.75	-2.75	0.24	0.24	0.08	0.08	1.28	1.28
X'_{uu}	-12.49	-51.61	12.90	-11.98	28.28	67.80	36.39	46.00
X'_{uuu}	-11.57	-11.57	19.80	19.80	49.66	49.66	59.55	59.55
X'_{vv}	-8.20	-8.20	-8.13	-8.13	-15.47	-15.47	-15.51	-15.51
X'_{rr}	44.90	-26.52	45.49	88.61	108.69	70.18	108.91	169.33
X'_{rv}	6.09	6.09	6.03	6.03	12.59	12.59	12.60	12.60
X'_{dd}	4.72	10.10	1.04	8.17	3.91	-12.01	1.80	1.89
X'_{udd}	9.27	9.27	0.06	0.06	7.92	7.92	2.30	2.30
X'_{vd}	3.38	-28.80	2.65	-26.15	1.44	-20.91	0.83	51.12
X'_{uvd}	3.77	-20.29	0.89	16.20	-15.92	-24.16	-18.83	7.14

Table 4.12: Comparison of identified hydrodynamic coefficients in surge motion in different wind directions

	Deviation(%) (-45°)				Deviation(%) (-90°)			
	LS	LS+GA	SVM	SVM+GA	LS	LS+GA	SVM	SVM+GA
Y'_{v}	0.26	0.26	0.26	0.26	-0.47	-0.47	-0.35	-0.35
Y'_{r}	0.05	0.05	0.06	0.06	-0.66	-0.66	-0.59	-0.59
Y'_{vvv}	-0.93	-0.93	-0.92	-0.92	-7.66	-7.66	-7.53	-7.53
Y'_{vvr}	-1.08	-1.08	-1.08	-1.08	2.82	2.82	2.78	2.78
Y'_{vu}	9.15	9.15	9.14	9.14	-9.07	-9.07	-8.43	-8.43
Y'_{ru}	7.75	7.75	7.71	7.71	-9.76	-9.76	-9.27	-9.27
Y'_{d}	0.34	0.34	0.33	0.33	0.23	0.23	0.13	0.13
Y'_{ddd}	-0.67	-33.48	-0.65	32.98	-7.26	-7.26	-7.24	-7.24
Y'_{ud}	4.03	4.03	4.00	4.00	-1.66	-1.66	-2.16	-2.16
Y'_{uud}	38.14	38.14	37.94	37.94	-42.95	-25.10	-45.76	-26.22
Y'_{vdd}	120.46	208.19	119.59	218.53	153.03	204.88	138.93	162.83
Y'_{vvd}	-4.14	-4.14	-4.01	-4.01	11.04	11.04	11.25	11.25
Y'_{0}	44.51	-11.40	43.75	33.08	26.94	-21.99	29.59	22.86
Y'_{0u}	-14.78	-46.11	-14.92	-2.62	-277.74	-320.48	-263.71	-243.49
Y'_{0uu}	-359.39	-269.87	-352.30	-430.44	-1845.97	-1977.08	-1774.34	-1956.72
	Deviation(%) (45°)				Deviation(%) (90°)			
	LS	LS+GA	SVM	SVM+GA	LS	LS+GA	SVM	SVM+GA
Y'_{v}	-0.06	-0.06	-0.09	-0.09	0.48	0.48	0.39	0.39
Y'_{r}	0.08	0.08	0.07	0.07	0.68	0.68	0.62	0.62
Y'_{vvv}	-1.61	-1.61	-1.59	-1.59	-9.37	-9.37	-9.36	-9.36
Y'_{vvr}	-1.01	-1.01	-1.00	-1.00	4.26	4.26	4.25	4.25
Y'_{vu}	7.29	7.29	7.07	7.07	-11.44	-11.44	-11.86	-11.86
Y'_{ru}	7.83	7.83	7.60	7.60	-11.82	-11.82	-12.09	-12.09
Y'_{d}	0.03	0.03	0.06	0.06	-1.34	-1.34	-1.24	-1.24
Y'_{ddd}	0.27	-46.35	0.28	-18.13	-3.78	-3.78	-3.81	-3.81
Y'_{ud}	4.35	4.35	4.52	4.52	-5.63	-5.63	-5.15	-5.15
Y'_{uud}	46.18	46.18	47.01	47.01	-60.32	-50.49	-56.95	-40.43
Y'_{vdd}	135.91	249.41	134.65	25.21	54.02	115.22	50.30	-24.53
Y'_{vvd}	-2.23	-2.23	-2.02	-2.02	23.31	23.31	22.99	22.99
Y'_{0}	-40.71	-40.63	-43.60	-33.08	-37.35	-12.89	-40.93	-24.39
Y'_{0u}	9.05	1.17	6.05	1.94	212.72	313.27	202.45	85.45
Y'_{0uu}	117.48	106.48	83.30	61.93	1170.52	1644.29	1103.99	749.53

Table 4.13: Comparison of identified hydrodynamic coefficients in sway motion in different wind directions

	Deviation(%) (-45°)				Deviation(%) (-90°)			
	LS	LS+GA	SVM	SVM+GA	LS	LS+GA	SVM	SVM+GA
N'_v	-0.28	-0.28	-0.31	-0.31	-0.26	-0.26	-0.02	-0.02
N'_r	-0.23	-0.23	-0.25	-0.25	-0.57	-0.57	-0.44	-0.44
N'_{vvv}	-2.13	-2.13	-2.07	-2.07	18.56	18.56	18.32	18.32
N'_{vvr}	2.43	2.43	2.42	2.42	-3.29	-3.29	-3.26	-3.26
N'_{vu}	23.75	23.75	23.59	23.59	-9.97	-9.97	-8.95	-8.95
N'_{ru}	15.93	15.93	15.79	15.79	-8.64	-8.64	-8.13	-8.13
N'_d	-0.37	-0.37	-0.39	-0.39	-0.25	-0.25	-0.16	-0.16
N'_{ddd}	0.99	49.24	0.92	22.68	5.43	-5.32	5.47	26.19
N'_{ud}	-2.41	-2.41	-2.43	-2.43	-0.28	-0.28	0.07	0.07
N'_{uud}	-35.27	-35.27	-35.19	-35.19	20.80	20.80	23.03	23.03
N'_{vdd}	-27.91	-48.34	-27.71	-37.24	-31.56	-6.86	-30.03	-39.87
N'_{vvd}	16.51	16.51	16.41	16.41	-12.61	-12.61	-12.91	-12.91
N'_0	-27.51	-5.72	-27.73	-3.44	-24.81	-13.65	-24.66	-8.41
N'_{0u}	-23.62	-42.57	-22.41	-44.48	145.07	158.96	137.74	35.28
N'_{0uu}	19.94	47.52	29.42	5.91	987.48	1301.31	949.72	693.43
	Deviation(%) (45°)				Deviation(%) (90°)			
	LS	LS+GA	SVM	SVM+GA	LS	LS+GA	SVM	SVM+GA
N'_v	0.37	0.37	0.26	0.26	0.09	0.09	0.04	0.04
N'_r	0.47	0.47	0.41	0.41	0.14	0.14	0.11	0.11
N'_{vvv}	10.25	10.25	10.20	10.20	6.81	6.81	6.80	6.80
N'_{vvr}	-1.46	-1.46	-1.48	-1.48	-2.58	-2.58	-2.56	-2.56
N'_{vu}	-1.83	-1.83	-2.43	-2.43	-16.83	-16.83	-16.99	-16.99
N'_{ru}	-1.34	-1.34	-1.66	-1.66	-11.88	-11.88	-11.91	-11.91
N'_d	0.46	0.46	0.42	0.42	0.51	0.51	0.47	0.47
N'_{ddd}	0.58	-16.63	0.59	-14.02	2.55	-25.44	2.51	26.08
N'_{ud}	-1.58	-1.58	-1.85	-1.85	3.63	3.63	3.47	3.47
N'_{uud}	-13.15	-13.15	-14.73	-14.73	40.94	40.94	39.67	39.67
N'_{vdd}	-4.92	17.70	-4.75	27.73	8.48	-34.40	8.92	-5.91
N'_{vvd}	-11.95	-11.95	-11.98	-11.98	-11.71	-11.71	-11.45	-11.45
N'_0	9.02	-2.44	10.28	18.91	3.73	17.04	3.35	-19.07
N'_{0u}	-51.52	-42.46	-47.93	-62.84	-57.81	-38.88	-55.96	-76.69
N'_{0uu}	-380.71	-324.11	-351.23	-406.44	-290.56	-296.26	-279.05	-348.39

Table 4.14: Comparison of identified hydrodynamic coefficients in yaw motion in different wind directions

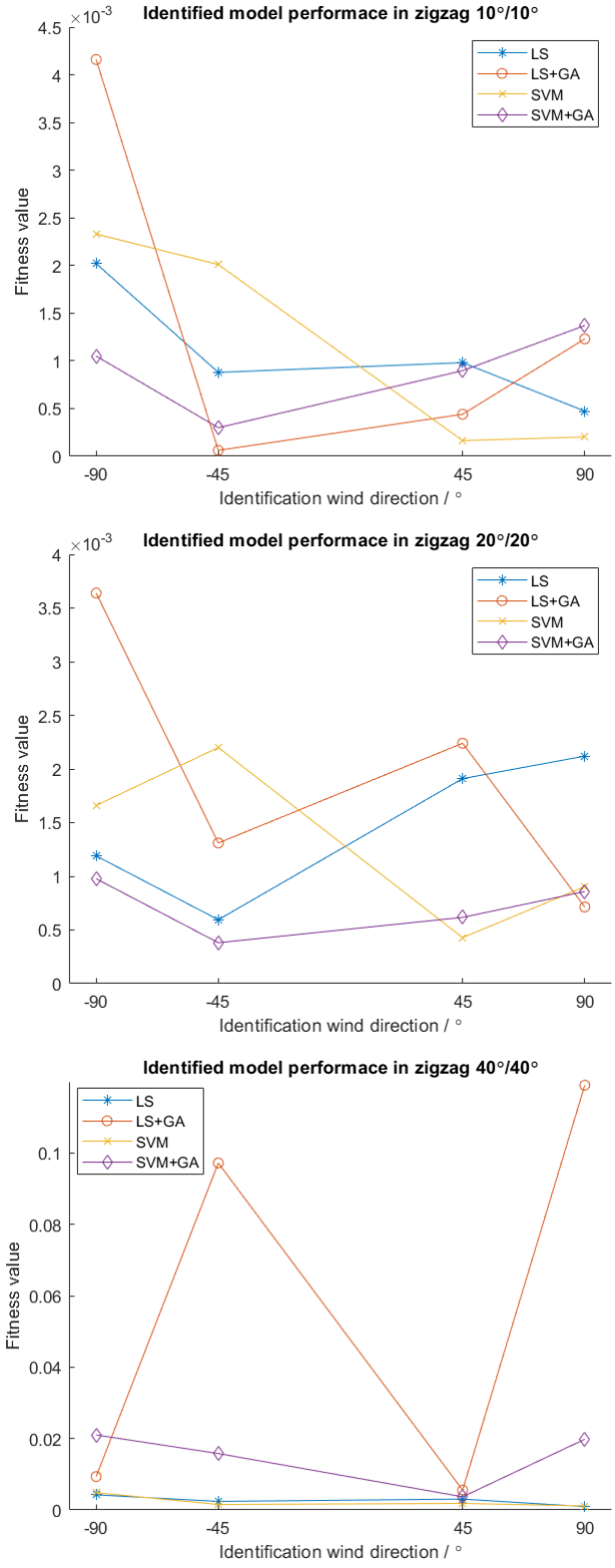

Figure 4.3: System performance comparison three

4.3 Validation of Identification Results

In the above studies, the identification results are verified by the benchmarks, and the low fitness values in system identification comparison also indicate the good accuracy of obtained results. A more intuitive way to validate the identification results is by trajectory comparison. 3 sets of extreme identification results of LS+GA and SVM+GA are selected for validation in zigzag 30/30, turning test and a random manoeuvre. based on the previous analyses, which include case of 16m/s in Section 4.2.1, case of -10% in Section 4.2.2 and case of -90°in Section 4.2.3. Besides, the simulation is performed under calm water condition. The trajectories comparisons are presented in the figure 4.4-4.6 for case 1, 4.7-4.9 for case 2 and 4.10-4.12 for case 3.

As shown in the figures, the generated trajectories on the left hand side, as well as the corresponding velocities components on the right hand side of both LS+GA and SVM have good agreement with the original ones in all the cases, which further proves the reliability of the identified hydrodynamic coefficients and the corresponding manoeuvring models. Even though the turning test of SVM+GA in case 2 has a distinct deviation from the true value, it's considered as acceptable given the fact that the hydrodynamic coefficients computed are able to reproduce the main characteristics in various ship behaviours when identification accuracy is degraded by wind with high noise. Same explanation is applied in random test of LS+GA in case 2.

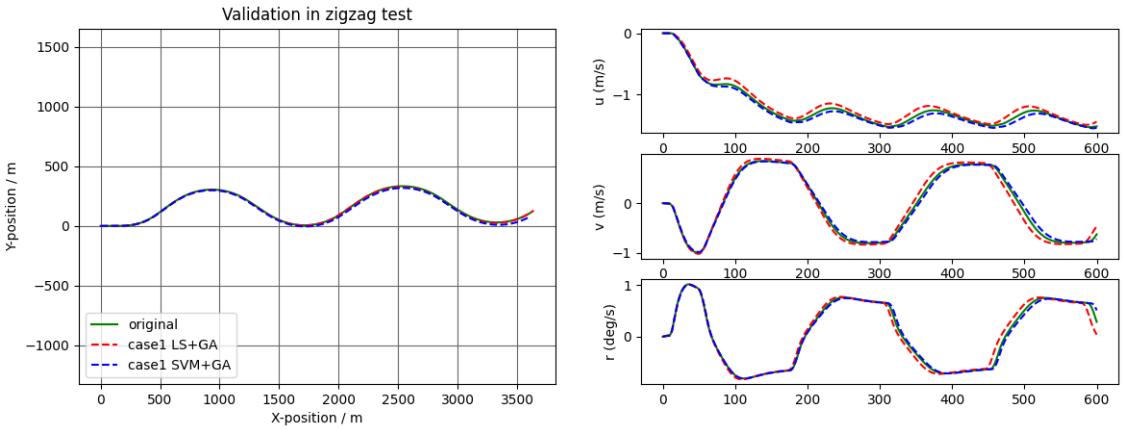

Figure 4.4: Validation of case 1—— zigzag test

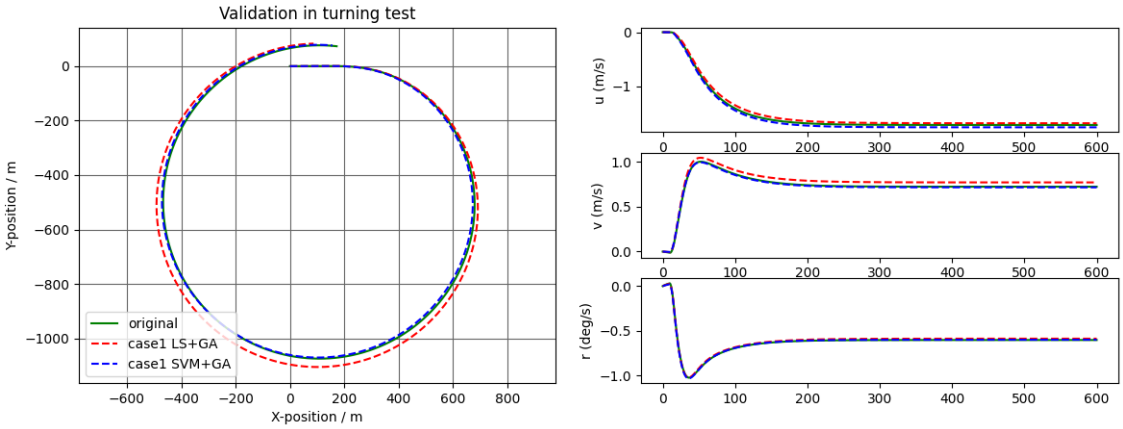

Figure 4.5: Validation of case 1—— turning test

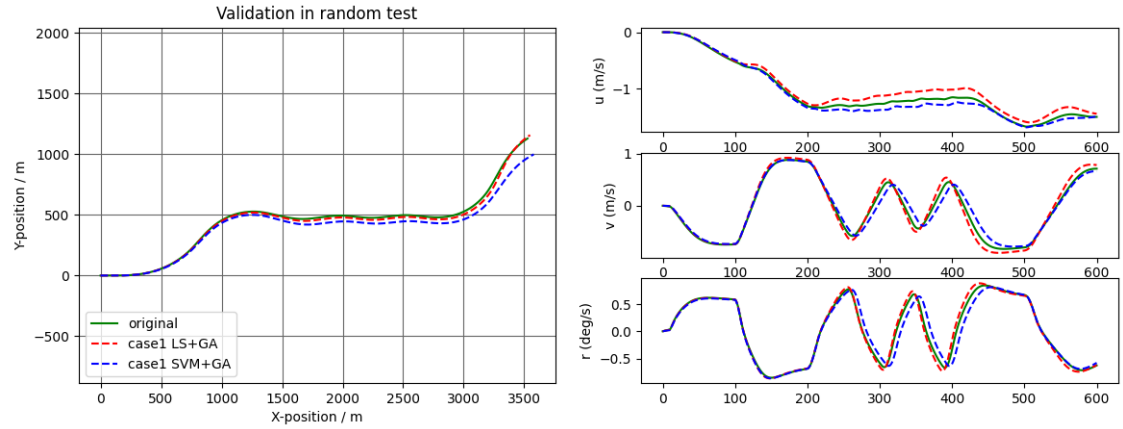

Figure 4.6: Validation of case 1—— random test

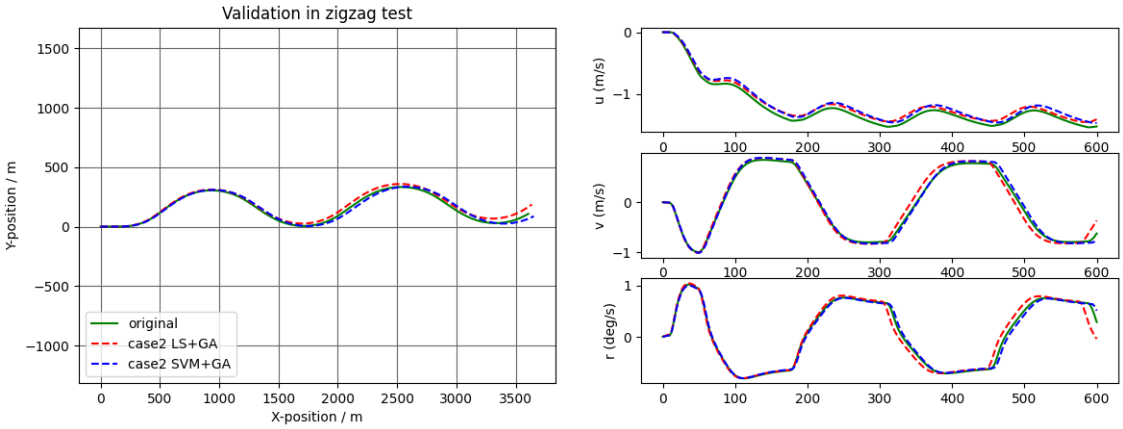

Figure 4.7: Validation of case 2—— zigzag test

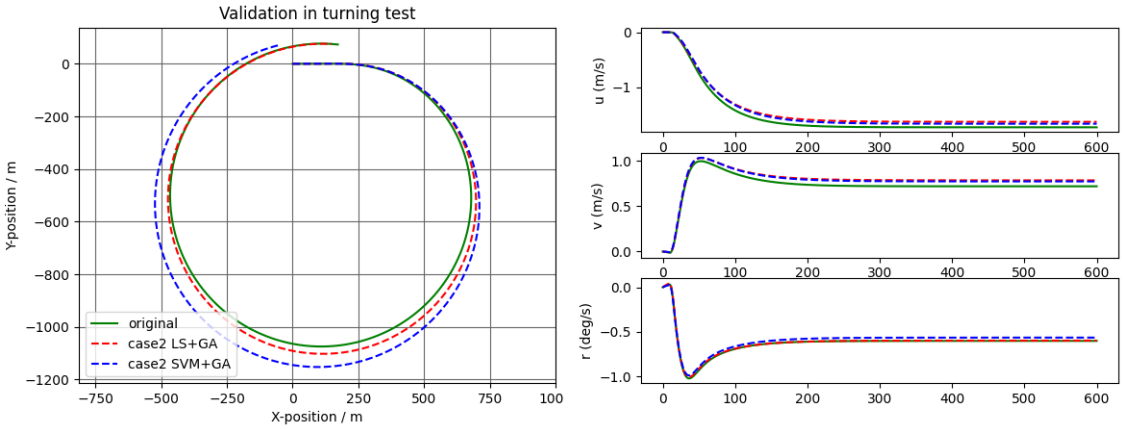

Figure 4.8: Validation of case 2—— turning test

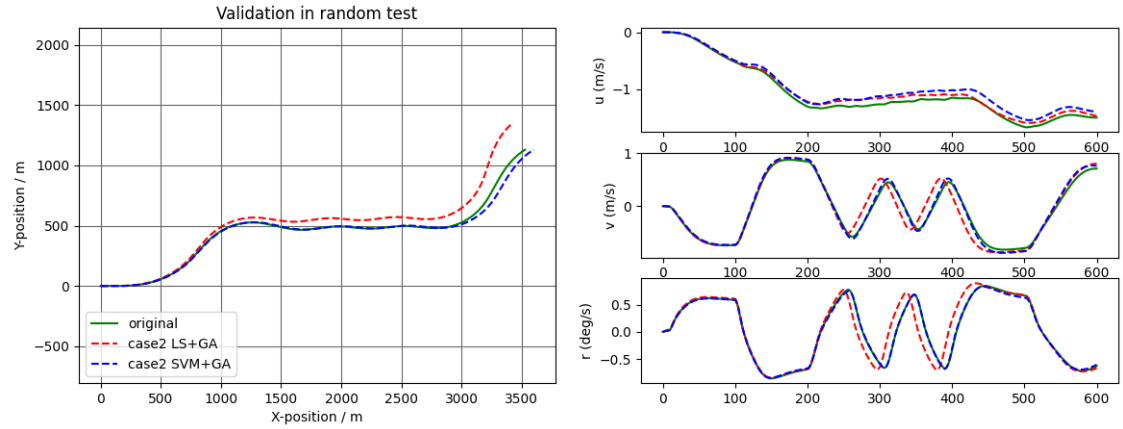

Figure 4.9: Validation of case 2—— random test

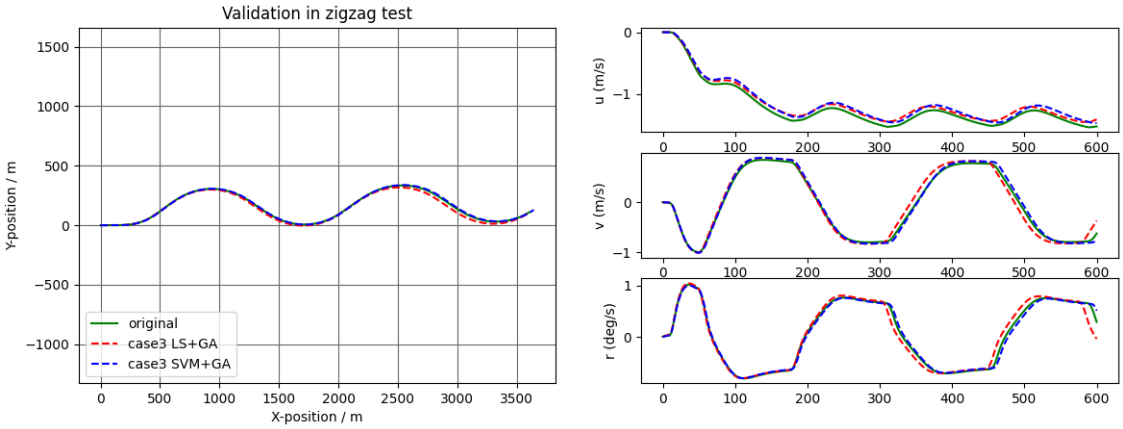

Figure 4.10: Validation of case 3—— zigzag test

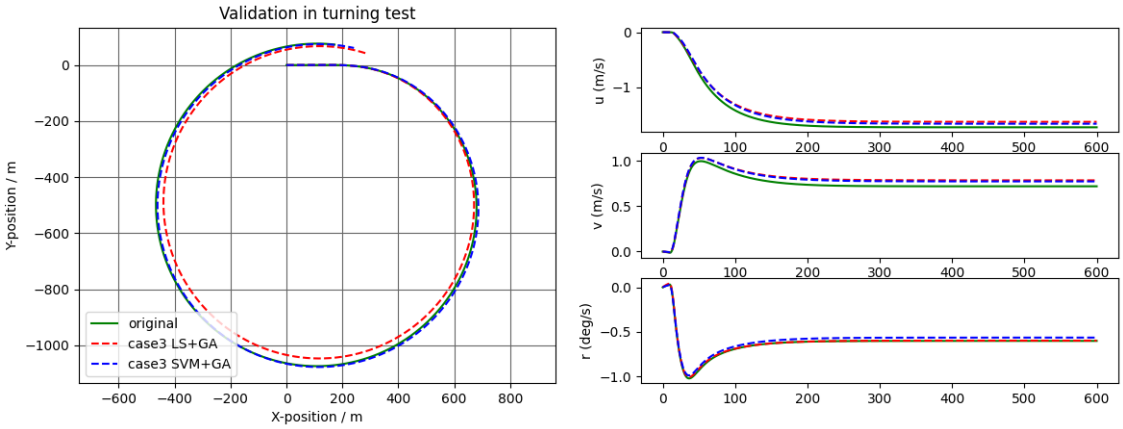

Figure 4.11: Validation of case 3—— turning test

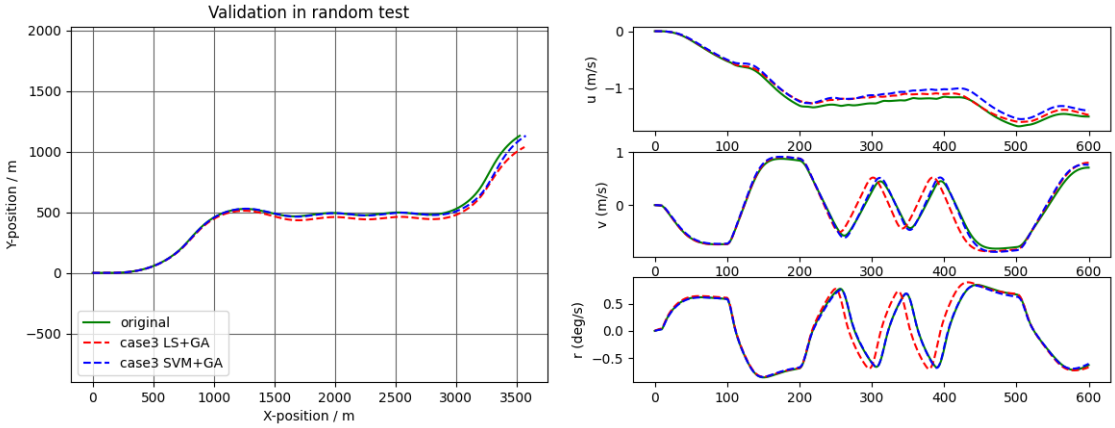

Figure 4.12: Validation of case 3—— random test

Chapter 5

Discussion

Chapter 5 focus on the evaluation of evolutionary optimization-based identification framework. Remark is made on the positive outcome, drawback as well as potential for future development with regard to the sensitivity analysis in section one. Besides, several reasons are listed in section two to explain why the performance of optimization method is less satisfying than expected. Furthermore, the method of LS+GA and SVM+GA are further discussed in section three on effectiveness, applicability and robustness. Last but not least, in section four, the environmental effects are discussed with respect to the accuracy of identified hydrodynamic coefficients.

5.1 Discussion of Sensitivity Analysis

In real application, the priori knowledge of hydrodynamic coefficients is hardly available for vessel models to be identified, and it's also not practical to optimize 40 or even more coefficients simultaneously. Therefore it's necessary to find a useful way to determine to select and group those coefficients which are in need of optimization and this is where sensitivity analysis comes into play in this paper. Looking back the experiments conducted in Chapter 4, one can find that SA is capable of locating the less accurate hydrodynamic coefficients with high deviations in most of cases, especially in sway and yaw motion, such as Y'_{vdd}, Y'_{0uu} and N'_{0uu}. In addition, in some more extreme cases, such as case of wind speed 16m/s, case of $\pm$ 10% noise, case of wind direction $\pm$ 90°, it's also able to capture X'_{rr}, Y'_0, Y'_{0u}, N'_{0u} and Y'_{uud}. The successfully picking up the right hydrodynamic coefficients is an positive sign of the employment of sensitivity analysis under the framework, which provides effective support for the optimization later.

Nevertheless, the shortcoming of SA still exists that it doesn't provide any direct information related to the accuracy of parameters other than their relative

importance in the model equation, which might result in unsatisfying selection, for instance, coefficient X'_{dd}, X'_{vd}, Y'_{ddd} and N'_{ddd} already have low deviations, but they are selected because sensitivity analysis only recognized their relative importance not the precision.

To improve the performance of SA, one of the possible approaches is to take into account the correlation matrix of input variables since collinearity is the main reason for parameter drift when noise presents, but this kind of analysis process is complicated and time consuming, which is more suitable for independent research later.

5.2 Discussion of Genetic Algorithm

Obviously, the estimation results computed by either LS or SVM method are affected by the environmental disturbance, especially in high wind, high noise level or large wind direction case, for which an optimization method based on genetic algorithm is employed in this study. In many of the experiments, there are about $\frac{1}{3}$ of selected hydrodynamic coefficients from SA which can be optimized to a better value during the process, while the others stay unchanged or become even worse. Ideally, GA should be able to improve the accuracy of all the selected hydrodynamic coefficients regardless of the cases, however, this is hard to achieve in practice considering three major limitations of GA.

The first one is generation number. The computation time increases significantly along with generation number and 200 generations require 3-4 hours to complete. To increase the generation number is very likely to improve the outcome ,but at the same time there is more cost on time, which is not an issue for offline identification but the other way around for online identification. Second limitation relates to the training data. The optimization results depends upon the richness of training data, and in order to have a better optimization, training data should contain as many characteristics of ship behaviour as possible, which could result in a huge-sized data set and more computation time required. Last limitation is the inherent feature of GA, which is its randomness. The search of optimal solution of GA is randomly proceeded, and it could lead to wrong evolution with sacrifice of some coefficients (as shown in surge motion).

Although issues mentioned above can't be resolved entirely, efforts in the later research are worth putting into smarter combination of simulation, data processing and identification so that the data can be constantly updated for estimation and optimization phase without large storage and long processing time. Additionally, other more complicated evolutionary algorithm are also worth testing in the future experiments.

5.3 Discussion of LS+GA and SVM+GA

The identification ability of LS or SVM method is highly promising in cases when wind speed and noise level are both low. The optimization is not actually needed under such mild condition where deviations of hydrodynamic coefficients are relatively low and system performance of the identified model is not largely affected by the inaccuracy coefficient-wise. A perfect example is SVM+GA in the case of 4m/s and 8m/s where the fitness value is very close to the stoping criterion 1e-5, and a better solution is challenging to find within 200 generations. As for LS+GA, even though the fitness value is decreased during the process, only limited optimization effect is shown in terms of coefficients, such as deviation of X'_{rr} from 20.35% to 10.09% in the case of 4m/s while some coefficients become worse than before such as deviation of X'_{vd} from 1.48% to 11.61% and Y'_{ddd} from -0.44% to -15.31%. But more positive effect of optimization can be found in the case of 8m/s where X'_{uu} is improved from -32.82% to -28.27%, X'_{uuu} from -54% to -40.98%, Y'_{0u} from 41.64% to 15.04% and Y'_{0uu} from 326.28% to 130.66%.

In the cases under hostile condition such as high wind speed, LS+GA and SVM+GA play a more effective role in obtaining better optimization results. Both LS+GA and SVM+GA perform well in the case of 12m/s and 16m/s. LS+GA is able to improve the results in both sway and yaw motion in the case of 12m/s, such as deviation of Y'_{0u} from 9.05% to 1.17%, Y'_{0uu} from 117.48% to 106.48%, N'_{0u} from -51.52% to -42.46% and N'_{0uu} from -380.71% to -324.11%. Additionally, SVM+GA improves deviation of Y'_{vdd} from 134.65% to 25.21%, Y'_0 from -43.60 to -33.08, Y'_{0u} from 6.05% to 1.94%, Y'_{0uu} from 83.30% to 61.93% in the case of 12m/s and Y'_{0uu} from -657.54% to -558.04% as well as N'_{0uu} from -214.78% to -179.40%. Positive results can also be found in case of $\pm$ 10% noise for LS+GA and SVM+GA, but in case of large wind direction, only SVM+GA performs quite remarkably with deviations of Y'_{0u} optimized from 202.45% to 85.45%, Y'_{0uu} from 1103.99% to 749.5% in the case of 90°and deviations of N'_{0u} from 137.74% to 35.28% and N'_{0uu} from 949.72% to 693.43% in the case of -90°.

The effectiveness of LS+GA and SVM+GA might not be as satisfying as expected in terms of improvement on hydrodynamic coefficients, and there is certainly badness encountered as well. But on the other hand, the optimization does show up in different cases. What's more, it can be also reflected from the system performance in cases such as wind speed 16m/s, noise level 10%, wind direction -90°, -45°where SVM+GA peaks the performance in simulated zigzag 20°20°, and in cases such as wind direction -45°and 90°where LS+GA beats the rest in simulated zigzag 10°/10°and 20°/20°respectively. Furthermore, the validation also demonstrates that the manoeuvring model identified by LS+GA and SVM+GA has good agreement with original one in terms of trajectory and velocity. In fact, the judgement of whether the method is useful or not is not easy to make when

there is no absolute improvement or degradation in comparison, and in reality, the goodness of the identified coefficients is most likely validated by performing manoeuvring simulation when there's no benchmark or prior knowledge. Therefore, the more meaningful issue is to find out when or where to use the method based on the current founding. The table 5.1 specifies the effective and applicable scenarios for LS+GA and SVM+GA, represented by O and $\Diamond$ respectively. sign - means no such scenarios and sign $\times$ means none of the method is suitable.

Noise level \ Wind speed	4m/s	8m/s	12m/s	16m/s
-10%	-	-	O $\Diamond$	-
-5%	$\times$	$\times$	O $\Diamond$	$\Diamond$
5%	-	-	O $\Diamond$	-
10%	-	-	O $\Diamond$	-

(a)

Wind direction \ Wind speed	4m/s	8m/s	12m/s	16m/s
-90°	-	-	$\Diamond$	-
-45°	-	-	O $\Diamond$	-
45°	$\times$	$\times$	O $\Diamond$	O $\Diamond$
90°	-	-	$\Diamond$	-

(b)

Table 5.1: Effective and applicable scenarios for LS+GA(O) and SVM+GA($\Diamond$)

5.4 Discussion of Environmental Effects

The accuracy of identification results is subjected to the wind disturbances. When it comes to the experiment of wind speed, it can be seen that some of the hydrodynamic coefficients are more sensitive to certain conditions than the others. For instance, in the case of 4m/s and 8m/s, X'_{uu} and X'_{uuu} are several dozens percent from the true values while their deviations become relatively low in the case of 12m/s and 16m/s. Besides, a few hydrodynamic coefficients are pretty accurately identified regardless of the wind speed, such as X'_u, Y'_u, Y'_r, Y'_d, N'_u, N'_r, N'_d. Furthermore, although there is variation in the coefficients, the model performance decreases along with higher wind speed without the presence of optimization.

As for noise level, the deviation of estimated hydrodynamic coefficients by LS or SVM has a linear relation with regard to noise level as observed from the table

4.9-4.11, which is not a good news for those with high deviations such as X'_{rr}, Y'_{vdd}, Y'_{0uu}, N'_{0u} and N'_{0uu}. But the ±10% is rather high in the experiment which doesn't often happen in real case. Besides, one thing worth mentioning is that the noise defined here is more similar to a system error in the measurement, and the reason for doing so is to better compare the effect of different noise levels with a quantitive magnitude. In the future study, a Gaussian white noise might be a better solution for simulating the noise generation.

The wind direction has similar influence on the accuray of hydrodynamic coefficients in surge motion in the case of ±45°. In the sway motion, the estimated results of case of -45°is worse than those of 45°while in the yaw motion, it's the other way around. Moreover, in the case of ±90°, results estimated by LS or SVM become much worse. Even though the deviation of N'_{0uu} is relatively low in the case of 90°compared with other cases, the deviations of Y'_{0uu} is as extremely high as 1170.52% in LS and 1103.99% in SVM. Wind direction of -90°has large impact on the results where accuracy in all 3-DOF is low in many hydrodynamic coefficients, especially Y'_{0uu} and N'_{0uu}.

Chapter 6

Conclusion and Future Work

Chapter 6 contains two sections, section one concludes the work of this master thesis, summarizing the useful outcome and new founding; section two is the future work suggested by author based on the previous discussions and research experiences gained during the master thesis period.

6.1 Conclusion

In this mater thesis, an identification method and evolutionray optimization framework is proposed and investigated for parameter identification in ship manoeuvring under environmental disturbances induced by wind. Abkowitz model of a Mariner class cargo ship in 3-DOF is used and wind force and moment are taken into account for the identification model. The training data for identification is taken from simulation of 20-20 zigzag manoeuvre using MSS toolbox. The identification is conducted on various wind conditions with different wind speed, noise and direction using four methods, including least square method, support vector machine least, least square method + genetic algorithm and support vector machine method + genetic algorithm. By utilizing sensitivity analysis, importance ranking of the estimated hydrodynamic coefficients is computed, based on which 15 of them are selected for optimization using genetic algorithm based on defined fitness function.

The LS and SVM method can accurately identity most of the hydrodynamic coefficients under calm water and moderate wind condition, but the results of them suffer significantly from condition of high wind speed, high noise level or large direction, where some deviations of hydrodynamic coefficients from their true values become dramatically high. The method of LS+GA or SVM +GA is able to improve some of the selected coefficients to some extent under certain scenarios, but the overall effectiveness is not as satisfying as expected due to the limitations of

genetic algorithm and the robustness needs to be further improved. The reliability of hydrodynamic coefficients identified using LS+GA and SVM+GA method in three extreme cases is validated by trajectory and velocity comparison in zigzag 30°/30°test, turning test and random test.

6.2 Future Work

This master thesis starts a research in new method development in the field of parameter identification for ship manoeuvring model, and the mission of the research is not yet completed. There are several aspects which can be further investigated. First of all, the optimization performance of genetic algorithm will require more extra work to improve, and more generation numbers or multiple data set combination can be tested to find out their influence on the optimization results. Then, effectiveness of sensitivity analysis can studied in combination of correlation matrices of input variables of identification model. Furthermore, one can also carry out more analysis in more wind speeds, noise levels and wind directions, and make it more complicated, dynamic wind speed and direction can also considered. Last but not least, the velocity inputs can be polluted with measurement noise in the future study and identification is conducted using the polluted measurement data.

Apart from the continuing work of this master thesis, there is one more potential research case suggested. Some of the ship hydrodynamic coefficients might change in the marine operation such as cargo loading and unloading, and therefore it will be interested to study such effect by performing parameter identification.

Bibliography

[Aarts, 2012] Aarts, R. (2012). System identification and parameter estimation. Technical report, Universiteit Twente.

[Abkowitz, 1980] Abkowitz (1980). Measurement of hydrodynamic characteristics from ship maneuvering trials by system identification. *SNAME Transactions*, 88(Issue 1):283–318.

[Araki et al., 2012] Araki, M., Sadat-Hosseini, H., Sanada, Y., Tanimoto, K., Umeda, N., and Stern, F. (2012). Estimating maneuvering coefficients using system identification methods with experimental, system-based, and cfd free-running trial data. *Ocean Engineering*, 51:63–84.

[Artyszuk, 2018] Artyszuk, J. (2018). A study on the identi cation of the second-order linear nomoto model from the zigzag test.

[Avula, 2003] Avula, X. J. (2003). Mathematical modeling. In Meyers, R. A., editor, *Encyclopedia of Physical Science and Technology (Third Edition)*, pages 219–230. Academic Press, New York, third edition edition.

[Blendermann, 1994] Blendermann, W. (1994). Parameter identification of wind loads on ships. *Journal of Wind Engineering and Industrial Aerodynamics*, 51(3):339–351.

[Boser et al., 1992] Boser, B. E., Guyon, I. M., and Vapnik, V. N. (1992). A training algorithm for optimal margin classifiers. In *Proceedings of the Fifth Annual Workshop on Computational Learning Theory*, COLT '92, pages 144–152, New York, NY, USA. Association for Computing Machinery.

[Cai et al., 2011] Cai, G., Chen, B. M., and Lee, T. H. (2011). *Coordinate Systems and Transformations*, pages 23–34. Springer London, London.

[Chen and Ljung, 2013] Chen, T. and Ljung, L. (2013). Implementation of algorithms for tuning parameters in regularized least squares problems in system identification. *Automatica*, 49(7):2213 – 2220.

[Chislett and Strom-Tejsen, 1965] Chislett, M. S. and Strom-Tejsen, J. (1965). Planar motion mechanism tests and full-scale steering and manoeuvring predictions for a mariner class vessel. 12:201–224.

[DNV, 2019] DNV (2019). New digital twin concept could show real-time status of safety risk and operations.

[Drucker et al., 1997] Drucker, H., Burges, C. J. C., Kaufman, L., Smola, A., and Vapnik, V. (1997). Support vector regression machines. In Mozer, M. C., Jordan, M., and Petsche, T., editors, *Advances in Neural Information Processing Systems*, volume 9. MIT Press.

[Fossen, 2011] Fossen, T. I. (2011). *Handbook of Marine Craft Hydrodynamics and Motion Control*. John Wiley & Sons, Ltd.

[Fossen and Perez, 2004] Fossen, T. I. and Perez, T. (2004). Marine systems simulator (mss).

[Fujiwara and Nimura, 2005] Fujiwara, T. and Nimura, T. (2005). New estimation method of wind forces acting on ships on the basis of mathematical model.

[Gad, 2021] Gad, A. F. (2021). Pygad: An intuitive genetic algorithm python library.

[Hayes, 1971] Hayes, M. N. (1971). *Parametric Identification of Nonlinear Stochastic Systems Applied to Ocean Vehicle Dynamics*. PhD thesis, Massachusetts Institute of Technology.

[H.T.Banks, 1989] H.T.Banks, K. (1989). *Estimation Techniques for Distributed Parameter Systems*. Birkhäuser Boston.

[Hwang, 1980] Hwang, W. (1980). *Application of system identification to ship maneuvering*. PhD thesis, Massachusetts Institute of Technology.

[Isakov, 1990] Isakov, V. (1990). *Inverse Problems for Partial Differential Equations*. Applied Mathematical Sciences. Springer, New York, NY.

[Islam and Guedes Soares, 2018] Islam, H. and Guedes Soares, C. (2018). Estimation of hydrodynamic derivatives of a container ship using pmm simulation in openfoam. *Ocean Engineering*, 164.

[ITTC, 2002] ITTC (2002). Full scale manoeuvring trials procedure.

[Jian-Chuan et al., 2015] Jian-Chuan, Y., Zao-Jian, Z., and Feng, X. (2015). Parametric Identification of Abkowitz Model for Ship Maneuvering Motion by Using Partial Least Squares Regression. *Journal of Offshore Mechanics and Arctic Engineering*, 137(3). 031301.

[Kalman, 1960] Kalman, R. E. (1960). A new approach to linear filtering and prediction problems. *Transactions of the ASME–Journal of Basic Engineering*, 82(Series D):35–45.

[Liu et al., 2019] Liu, Y., Zou, L., and Zou, Z.-J. (2019). Computational fluid dynamics prediction of hydrodynamic forces on a manoeuvring ship including effects of dynamic sinkage and trim. *Proceedings of the Institution of Mechanical Engineers, Part M: Journal of Engineering for the Maritime Environment*, 233(1):251–266.

[Ljung, 1998] Ljung, L. (1998). System identification. *In: Procházka A., Uhlíř J., Rayner P.W.J., Kingsbury N.G. (eds) Signal Analysis and Prediction.*, pages 163–173.

[Luo et al., 2016] Luo, W., Guedes Soares, C., and Zou, Z. (2016). Parameter Identification of Ship Maneuvering Model Based on Support Vector Machines and Particle Swarm Optimization. *Journal of Offshore Mechanics and Arctic Engineering*, 138(3). 031101.

[Luo and Li, 2017] Luo, W. and Li, X. (2017). Measures to diminish the parameter drift in the modeling of ship manoeuvring using system identification. *Applied Ocean Research*, 67:9–20.

[Luo and Zhang, 2016] Luo, W. and Zhang, Z. (2016). Modeling of ship maneuvering motion using neural networks. *Journal of Marine Science and Application*, 15(4):426–432.

[Mahfouz, 2004] Mahfouz, A. (2004). Identification of the nonlinear ship rolling motion equation using the measured response at sea. *Ocean Engineering*, 31:2139–2156.

[Moeller, 2004] Moeller, D. P. F. (2004). *Parameter Identification of Dynamic Systems*, pages 257–310. Springer Berlin Heidelberg, Berlin, Heidelberg.

[Perera et al., 2015] Perera, L. P., Oliveira, P., and Guedes Soares, C. (2015). System Identification of Nonlinear Vessel Steering. *Journal of Offshore Mechanics and Arctic Engineering*, 137(3). 031302.

[Perera et al., 2016] Perera, L. P., Oliveira, P., and Guedes Soares, C. (2016). System identification of vessel steering with unstructured uncertainties by persistent excitation maneuvers. *IEEE Journal of Oceanic Engineering*, 41(3):515–528.

[Qin et al., 2014] Qin, Y., Li, J., Yong, M., Chi, S., and Zhang, L. (2014). Parametric identification of ship's maneuvering motion based on improved least square method. *2014 International Conference on Mechatronics, Electronic, Industrial and Control Engineering, MEIC 2014*, pages 779–784.

[Rajesh and Bhattacharyya, 2008] Rajesh, G. and Bhattacharyya, S. (2008). System identification for nonlinear maneuvering of large tankers using artificial neural network. *Applied Ocean Research*, 30(4):256 – 263.

[Rizzi and Ruggiero, 2013] Rizzi, G. and Ruggiero, M. (2013). *Relativity in Rotating Frames: Relativistic Physics in Rotating Reference Frames*. Fundamental Theories of Physics. Springer Netherlands.

[Ross et al., 2015] Ross, A., Hassani, V., Selvik, Ø., Ringen, E., and Fathi, D. (2015). Identification of Nonlinear Manoeuvring Models for Marine Vessels Using Planar Motion Mechanism Tests. In *International Conference on Offshore Mechanics and Arctic Engineering*, volume Volume 7: Ocean Engineering. V007T06A014.

[Saltelli, 2002] Saltelli, A. (2002). Sensitivity analysis for importance assessment. *Risk Analysis*, 22(3):579–590.

[Shi et al., 2009] Shi, C., Zhao, D., Peng, J., and Shen, C. (2009). Identification of ship maneuvering model using extended kalman filtering.

[SNAME, 1950] SNAME (1950). *Nomenclature for treating the motion of a submerged body through a fluid*. Technical and research bulletin No 1-5. Society of Naval Architects and Marine Engineers (SNAME), New York.

[Söderström, 2013] Söderström, T. (2013). Comparing some classes of bias-compensating least squares methods. *Automatica*, 49(3):840 – 845.

[Sohlberg and Jacobsen, 2008] Sohlberg, B. and Jacobsen, E. (2008). Grey box modelling – branches and experiences. *IFAC Proceedings Volumes*, 41(2):11415 – 11420. 17th IFAC World Congress.

[Sun and Wang, 2012] Sun, L. and Wang, D. (2012). Optimal structural design of the midship of a vlcc based on the strategy integrating svm and ga. *Journal of Marine Science and Application*, 11(1):59–67.

[Sutulo and Guedes Soares, 2014] Sutulo, S. and Guedes Soares, C. (2014). An algorithm for offline identification of ship manoeuvring mathematical models from free-running tests. *Ocean Engineering*, 79:10 – 25.

[Suykens et al., 2002] Suykens, J. A. K., Van Gestel, T., De Brabanter, J., De Moor, B., and Vandewalle, J. (2002). *Least Squares Support Vector Machines*. WORLD SCIENTIFIC.

[Suykens and Vandewalle, 1999] Suykens, J. A. K. and Vandewalle, J. (1999). Least squares support vector machine classifiers. *Neural Processing Letters*, 9(3):293–300.

[Wang et al., 2021] Wang, T., Li, G., Wu, B., Æsøy, V., and Zhang, H. (2021). Parameter identification of ship manoeuvring model under disturbance using support vector machine method. *Ships and Offshore Structures*, 0(0):1–9.

[Wang et al., 2013] Wang, X., Zou, Z., and Yin, J. (2013). Modular parameter identification for ship manoeuvring prediction based on support vector machines. In *The Twenty-third International Offshore and Polar Engineering Conference*, page 6, Anchorage, Alaska. International Society of Offshore and Polar Engineers.

[Wang et al., 2019] Wang, Z., Zou, Z., and Guedes Soares, C. (2019). Identification of ship manoeuvring motion based on nu-support vector machine. *Ocean Engineering*, 183:270–281.

[Wang and Zou, 2018] Wang, Z.-H. and Zou, Z.-J. (2018). Quantifying multicollinearity in ship manoeuvring modeling by variance inflation factor. Volume 7A: Ocean Engineering. V07AT06A001.

[Xie et al., 2020] Xie, S., Chu, X., Liu, C., Liu, J., and Mou, J. (2020). Parameter identification of ship motion model based on multi-innovation methods. *Journal of Marine Science and Technology*, 25(1):162–184.

[Xing and McCue, 2010] Xing, Z. and McCue, L. (2010). Modeling ship equations of roll motion using neural networks. *Naval Engineers Journal*, 122(Issue 3):49–60.

[Xu and Guedes Soares, 2016] Xu, H. and Guedes Soares, C. (2016). Vector field path following for surface marine vessel and parameter identification based on ls-svm. *Ocean Engineering*, 113:151 – 161.

[Xu and Guedes Soares, 2020] Xu, H. and Guedes Soares, C. (2020). Manoeuvring modelling of a containership in shallow water based on optimal truncated nonlinear kernel-based least square support vector machine and quantum-inspired evolutionary algorithm. *Ocean Engineering*, 195:106676.

[Xu et al., 2018a] Xu, H., Hassani, V., and Guedes Soares, C. (2018a). Parameters estimation of nonlinear manoeuvring model for marine surface ship based on pmm tests. In *International Conference on Offshore Mechanics and Arctic Engineering*, volume Volume 11B: Honoring Symposium for Professor Carlos Guedes Soares on Marine Technology and Ocean Engineering. V11BT12A010.

[Xu et al., 2018b] Xu, H., Hassani, V., and Guedes Soares, C. (2018b). Parameters estimation of nonlinear manoeuvring model for marine surface ship based on pmm tests. In *International Conference on Offshore Mechanics and Arctic Engineering*, volume Volume 11B: Honoring Symposium for Professor Carlos Guedes Soares on Marine Technology and Ocean Engineering. V11BT12A010.

[Xu and Soares, 2019] Xu, H. and Soares, C. G. (2019). Hydrodynamic coefficient estimation for ship manoeuvring in shallow water using an optimal truncated ls-svm. *Ocean Engineering*, 191:106488.

[Yoon and Rhee, 2003] Yoon, H. K. and Rhee, K. P. (2003). Identification of hydrodynamic coefficients in ship maneuvering equations of motion by estimation-before-modeling technique. *Ocean Engineering*, 30(18):2379 – 2404.

[Yuan, 2017] Yuan, Z. (2017). Lecture notes on ship manoeuvering. Technical report, University of Straclyde.

[Zadeh, 1962] Zadeh, L. A. (1962). From circuit theory to system theory. *Proceedings of the IRE*, 50(5):856–865.

[Zaojian, 2006] Zaojian, Z. (2006). Lecture notes on ship manoeuvering and seakeeping. Technical Report 13-15, Shanghai Jiao Tong University.

[Zhang and Zou, 2011] Zhang, X. and Zou, Z. (2011). Identification of abkowitz model for ship manoeuvring motion using ϵ-support vector regression. *Journal of Hydrodynamics*, 23(3):353–360.

Appendix A

Codes

A.1 Least Square Method

```
% Data input obtained from zigzag simulation

u = load(u_16.txt');
v = load(v_16.txt');
r = load(r_16.txt') *pi/180 ;
delta=load(delta.txt');
psi=load(psi.txt');


% Ship speed and parameter
U0 = 7.7175;
L = 160.93;
m  = 798e-5;
Iz = 39.2e-5;
xG = -0.023;
Xudot =  -42e-5;   Yvdot =  -748e-5;   Nvdot = 4.646e-5;
                   Yrdot =-9.354e-5;   Nrdot = -43.8e-5;

% Data processing
t_dot = 0.1;
m11 = m-Xudot;
m22 = m-Yvdot;
m23 = m*xG-Yrdot;
m32 = m*xG-Nvdot;
```

```
m33 = Iz-Nrdot;
detM22 = m22*m33-m23*m32;

U = sqrt((U0 + u).^2 + v.^2);
u1 = u ./U;
v1 = v ./ U;
r1 = r * L ./ U ;

% Noise generation
n1 = [-0.05,-0.1,-0.15,-0.2];
n2 = [0.05,0.1,0.15,0.2];


% Parameters for wind force calculation
v_w = 16;
v_p = v_w * ( 1+n1(1) )  ;
beta = 45*pi/180;
AFw       = 469;
ALw       = 1874;
Loa       = L;
sL        = 7.2;
sH        = 20.5;
vessel_no = 2;

% Wind force calculation and non-dimensionalization
u_r = u + v_p*cos(beta - psi);
v_r = v - v_p*sin(beta - psi);
V_r = sqrt((U0 + u_r).^2 + v_r.^2);
gamma_r = -atan2(v_r,U0 + u_r);
tau_wx = zeros(length(V_r),1);
tau_wy = zeros(length(V_r),1);
tau_wn = zeros(length(V_r),1);
for i = 1 : length(V_r)

    [tau_w,CX,CY,CK,CN] = blendermann94(gamma_r(i),V_r(i),AFw,ALw,sH,sL,Loa,vessel_

    tau_wx(i) = tau_w(1)/(1/2 * 1025 * L^2  *U(i) ^2);
    tau_wy(i) = tau_w(2)/(1/2 * 1025 * L^2  *U(i) ^2);
    tau_wn(i) = tau_w(3)/(1/2 * 1025 * L^3  *U(i) ^2);
```

```
end

% Velocity difference method

u_dot = (u(2:end) - u(1:end-1)) / t_dot;
v_dot = (v(2:end) - v(1:end-1)) / t_dot;
r_dot = (r(2:end) - r(1:end-1)) / t_dot;

% Input variables

AX =[u1 u1.^2 u1.^3 v1.^2 r1.^2 r1.*v1 delta.^2 u1.*delta.^2 v1.*delta u1.*v1.*del
AY =[v1 r1 v1.^3 v1.^2.*r1 v1.*u1 r1.*u1 delta delta.^3 u1.*delta ...
    u1.^2.*delta v1.*delta.^2  v1.^2.*delta ones(size(u1)) u1 u1.^2];
AN =[v1 r1 v1.^3 v1.^2.*r1 v1.*u1 r1.*u1 delta delta.^3 u1.*delta ...
    u1.^2.*delta v1.*delta.^2  v1.^2.*delta ones(size(u1)) u1 u1.^2];

X_X = AX(1:end-1,:);
X_Y = AY(1:end-1,:);
X_N = AN(1:end-1,:);

U_0 = U(1:end-1,1);

% Identification equation
y_X = (u_dot * L * m11 )./ U_0.^2 - tau_wx(1:end-1);
y_Y = ( m22 * v_dot + m23 * r_dot * L) * L ./ U_0.^2 -tau_wy(1:end-1) ;
y_N = ( m32 * v_dot + m33 * r_dot * L) * L ./ U_0.^2 -tau_wn(1:end-1);

% Least square method
aX = lsqminnorm(X_X,y_X);
aY = lsqminnorm(X_Y,y_Y);
aN = lsqminnorm(X_N,y_N);
```

A.2 Support Vector Machine Method

```
from sklearn import svm
import math
import numpy as np
import pandas as pd
```

```
from wind_force import windforce

class parameter_identification:

    def SVM_method(self):

        # Data input
        mariner = pd.read_excel(".xlsx", sheet_name='')
        self.u = mariner['u']
        self.v = mariner['v']
        self.r = mariner['r']
        self.delta = mariner['delta']
        self.psi = mariner['psi']
        self.u = np.ravel(self.u)
        self.v = np.ravel(self.v)
        self.r = np.ravel(self.r) * math.pi / 180

        # Ship speed and parameter
        U0 = 7.7175
        self.L = 160.93
        self.m = 798e-5
        self.Iz = 39.2e-5
        self.xG = -0.023
        self.Xudot = -42e-5
        self.Yvdot = -748e-5
        self.Yrdot = -9.354e-5
        self.Nvdot = 4.646e-5
        self.Nrdot = -43.8e-5
        self.m11 = self.m - self.Xudot
        self.m22 = self.m - self.Yvdot
        self.m23 = self.m * self.xG - self.Yrdot
        self.m32 = self.m * self.xG - self.Nvdot
        self.m33 = self.Iz - self.Nrdot

        # Data processing
        t_dot = 0.1
        self.U = np.sqrt((U0 + self.u)**2 +self.v**2)
        self.u_o = self.u
        self.v_o = self.v
        self.r_o = self.r
```

```
self.w = np.empty((len(self.psi),3))

# Noise generation
n1 = [-0.05, -0.1, -0.15, -0.2]
n2 = [0.05, 0.1, 0.15, 0.2]
# Parameter for wind force calculation
v_w = 12
v_p = v_w = 12 * (1 + n1[0])
beta = -90 * math.pi / 180
AFw = 469
ALw = 1874
Loa = self.L
sL = 7.2
# Wind force calculation and non-dimensionalization
for i in range(len(self.psi)):
  u_r = self.u_o[i] + v_p * math.cos(beta - self.psi[i])

  v_r = self.v_o[i] - v_p * math.sin(beta - self.psi[i])
  V_r = math.sqrt((U0 + u_r) ** 2 + v_r ** 2)
  gamma_r = -math.atan2(v_r, U0 + u_r)

  wind_force = windforce(gamma_r, V_r, AFw, ALw, Loa, sL)
  self.w[i,0] = wind_force[0] / (1 / 2 * 1025 * self.L ** 2 * self.U[i] **
  self.w[i,1] = wind_force[1] / (1 / 2 * 1025 * self.L ** 2 * self.U[i] **
  self.w[i,2] =  wind_force[2] / (1 / 2 * 1025 * self.L ** 3 * self.U[i] *

self.wx = self.w[:,0]
self.wy = self.w[:,1]
self.wn = self.w[:,2]

# Velocity difference method
self.u_dot = (self.u_o[1:] - self.u_o[:-1]) / t_dot
self.v_dot = (self.v_o[1:] - self.v_o[:-1]) / t_dot
self.r_dot = (self.r_o[1:] - self.r_o[:-1]) /  t_dot

self.u = self.u_o / self.U
self.v = self.v_o / self.U
self.r = self.r_o * self.L / self.U

# Input variables
```

```
        self.nx = np.array([self.u, self.u**2, self.u**3, self.v**2, self.r**2,
                                    self.r * self.v, self.delta**2,
                                    self.u * self.delta**2, self.v * self.delta,
                                    self.u * self.v * self.delta])
        self.ny = np.array([self.v, self.r, self.v**3, self.v**2 * self.r,
                                    self.v * self.u, self.r * self.u, self.delta
                                    self.delta**3, self.u * self.delta,
                                    self.u**2 * self.delta, self.v * self.delta*
                                    self.v**2 * self.delta, self.u, self.u**2])
        self.na = np.array([self.v, self.r, self.v**3, self.v**2 * self.r,
                                    self.v * self.u, self.r * self.u, self.delta
                                    self.delta**3, self.u * self.delta,
                                    self.u**2 * self.delta, self.v * self.delta*
                                    self.v**2 * self.delta, self.u, self.u**2])
        X_X = self.nx[:, :-1].T
        X_Y = self.ny[:, :-1].T
        X_N = self.na[:, :-1].T

        # Identification equation
        y_X = (self.u_dot * self.L * self.m11) / self.U[:-1]**2 -self.wx[:-1]
        y_Y = (self.m22 * self.v_dot + self.m23 * self.r_dot * self.L) * self.L /
         self.U[:-1]**2 -self.wy[:-1]
        y_N = (self.m32 * self.v_dot + self.m33 * self.r_dot * self.L) * self.L /
        self.U[:-1]**2 -self.wn[:-1]

        # SVM method
        lregr_x = svm.LinearSVR(tol=1e-6, C=1, max_iter=1e5)
        lregr_x.fit(X_X, y_X)
        pa_x = lregr_x.coef_
        lregr_y = svm.LinearSVR(tol=1e-6, C=1, max_iter=1e5)
        lregr_y.fit(X_Y, y_Y)
        pa_y = lregr_y.coef_
        pa_y = np.insert(pa_y, -2, lregr_y.intercept_)
        lregr_n = svm.LinearSVR(tol=1e-6, C=1,  max_iter=1e5)
        lregr_n.fit(X_N, y_N)
        pa_n = lregr_n.coef_
        pa_n = np.insert(pa_n, -2, lregr_n.intercept_)


activate = parameter_identification.SVM_method(parameter_identification)
```

A.3 Sensitivity Analysis

```
from SALib.sample import saltelli
from SALib.analyze import sobol
import numpy as np
import pandas as pd

# Input of estimated hydroynamic coefficients
coef1 = pd.read_csv('coefficients in surge.txt')
coef2 = pd.read_csv('coefficients in sway.txt')
coef3 = pd.read_csv('coefficients in yaw.txt')
coef1 = np.ravel(coef1)
coef2 = np.ravel(coef2)
coef3 = np.ravel(coef3)

problem1 = {
    'num_vars': 10,
    'names': ['u','u^2','u^3','v^2','r^2','r*v','d^2','u*d^2','v*d','u*v*d'],
    'bounds': [[0, 1],
               [0, 1],
               [0, 1],
               [0, 1],
               [0, 1],
               [0, 1],
               [0, 1],
               [0, 1],
               [0, 1],
               [0, 1]],
}

problem2 = {
    'num_vars': 14,
    'names': ['v', 'r', 'v^3', 'v^2*r', 'v*u', 'r*u', 'd', 'd^3', 'u*d', 'u^2*d',
              'v*d^2','v^2*d','u','u^2'],
    'bounds': [[0, 1],
               [0, 1],
               [0, 1],
```

```
                [0, 1],
                [0, 1],
                [0, 1],
                [0, 1],
                [0, 1],
                [0, 1],
                [0, 1],
                [0, 1],
                [0, 1],
                [0, 1],
                [0, 1]],
}
problem3 = problem2
# Generate samples
param_values1 = saltelli.sample(problem1, 5000)
Y1 = np.zeros([param_values1.shape[0]])
param_values2 = saltelli.sample(problem2, 5000)
Y2 = np.zeros([param_values2.shape[0]])
param_values3 = saltelli.sample(problem3, 5000)
Y3 = np.zeros([param_values2.shape[0]])

#Run models
for i, X in enumerate(param_values1):
    Y1[i] = coef1[0] * X[0] + coef1[1] * X[1] + coef1[2] * X[2] + coef1[3] * X[3] +
           coef1[4] * X[4] + coef1[5] * X[5] + coef1[6] * X[6] + coef1[7] * X[7] +
           coef1[8] * X[8] + coef1[9] * X[9]

for i, X in enumerate(param_values2):
    Y2[i] = coef2[0] * X[0] + coef2[1] * X[1] + coef2[2] * X[2] + coef2[3] * X[3] +
           coef2[4] * X[4] + coef2[5] * X[5] + coef2[6] * X[6] + coef2[7] * X[7] +
           coef2[8] * X[8] + coef2[9] * X[9] + coef2[10] * X[10] + coef2[11] * X[1
           coef2[13] * X[12] + coef2[14] * X[13]

for i, X in enumerate(param_values3):
    Y3[i] = coef3[0] * X[0] + coef3[1] * X[1] + coef3[2] * X[2] + coef3[3] * X[3] +
           coef3[4] * X[4] + coef3[5] * X[5] + coef3[6] * X[6] + coef3[7] * X[7] +
           coef3[8] * X[8] + coef3[9] * X[9] + coef3[10] * X[10] + coef3[11] * X[1
           coef3[13] * X[12] + coef3[14] * X[13]

# Perform analysis
```

```
Si_1 = sobol.analyze(problem1, Y1, print_to_console=True)
Si_2 = sobol.analyze(problem2, Y2, print_to_console=True)
Si_3 = sobol.analyze(problem3, Y3, print_to_console=True)
```

A.4 Genetic Algorithm

```
import pygad
import pandas as pd
import numpy as np
import ga_opt_trajectory1
# Input reference velcocity components
u_0 = pd.read_csv('LS/u_4.txt')
v_0 = pd.read_csv('LS/v_4.txt')
r_0 = pd.read_csv('LS/r_4.txt')
u_0 = np.ravel(u_0)
v_0 = np.ravel(v_0)
r_0 = np.ravel(r_0)
# Input estimated hydroynamic cofficients
df = pd.read_excel('GA_input_.xlsx',sheet_name='Sheet1')
coef = df.drop(df.columns[0], axis=1)
coef = np.array(coef)

# Fitness function definition
def fitness_fun(solution,solution_idx):
    t = ga_opt_trajectory1.zigzag([[0.], [0.], [0.], [0.], [0.], [0.], [0.]],
                                  0., 4000., 10., 0.1, [20., 20.], solution / 1e5)
    u = t[1]
    v = t[2]
    r = t[3]
    fitness = 40001 / (np.sum((u - u_0)**2) + np.sum((v - v_0)**2)
    + np.sum((r-r_0)**2))
    return fitness

# If performance is good enough, terminate the iteration
def my_on_generation(ga_instance):
    solution, solution_fitness, solution_idx = ga_instance.best_solution()
    print('one generation, solution_fitness = ',1/solution_fitness)
    # print('y solution is' ,solution[0:15]/1e5)
```

```
    # print('n solution is', solution[15:] / 1e5)
    if(solution_fitness> 100000 ):
        print('Generation=', ga_instance.generations_completed)
        return "stop"

# Initialization
my_initial_population = coef[:4] * 1e5

# GA settings
ga_instance = pygad.GA(num_generations=200,
                       num_parents_mating=4,
                       # num_genes=15,
                       fitness_func=fitness_fun,
                       crossover_probability=0.6,
                       parent_selection_type="rank",
                       keep_parents=3,
                       random_mutation_min_val=-1,
                       random_mutation_max_val=1,
                       mutation_probability=1,
                       mutation_type="random",
                       gene_space=[coef[0][0] * 1e5,
  {'low':  coef[0][1] * 1e5 * 1.5, 'high': coef[0][1] * 1e5 * 0.5},
  {'low':  coef[0][2] * 1e5 * 1.5, 'high': coef[0][2] * 1e5 * 0.5},
  coef[0][3] * 1e5,
  {'low':  coef[0][4] * 1e5 * 0.5, 'high': coef[0][4] * 1e5 * 1.5},
  coef[0][5] * 1e5,
  {'low':  coef[0][6] * 1e5 * 1.5, 'high': coef[0][6] * 1e5 * 0.5},
  coef[0][7] * 1e5,
  {'low':  coef[0][8] * 1e5 * 0.5, 'high': coef[0][8] * 1e5 * 1.5},
  coef[0][9] * 1e5,
  coef[0][10] * 1e5,
  coef[0][11] * 1e5,
  coef[0][12] * 1e5,
  coef[0][13] * 1e5,
  coef[0][14] * 1e5,
  coef[0][15] * 1e5,
  coef[0][16] * 1e5,
  {'low':  coef[0][17] * 1e5 * 1.5, 'high': coef[0][17] * 1e5 * 0.5},
  coef[0][18] * 1e5,
  coef[0][19] * 1e5,
```

```
  {'low':  coef[0][20] * 1e5 * 1.5, 'high': coef[0][20] * 1e5 * 0.5},
  coef[0][21] * 1e5,
  {'low':  coef[0][22] * 1e5 * 1.5, 'high': coef[0][22] * 1e5 * 0.5},
  {'low':  coef[0][23] * 1e5 * 1.5, 'high': coef[0][23] * 1e5 * 0.5},
  {'low':  coef[0][24] * 1e5 * 1.5, 'high': coef[0][24] * 1e5 * 0.5},
  coef[0][25] * 1e5,
  coef[0][26] * 1e5,
  coef[0][27] * 1e5,
  coef[0][28] * 1e5,
  coef[0][29] * 1e5,
  coef[0][30] * 1e5,
  coef[0][31] * 1e5,
  {'low':  coef[0][32] * 1e5 * 0.5, 'high': coef[0][32] * 1e5 * 1.5},
  coef[0][33] * 1e5,
  coef[0][34] * 1e5,
  {'low':  coef[0][35] * 1e5 * 0.5, 'high': coef[0][35] * 1e5 * 1.5},
  coef[0][36] * 1e5,
  {'low':  coef[0][37] * 1e5 * 0.5, 'high': coef[0][37] * 1e5 * 1.5},
  {'low':  coef[0][38] * 1e5 * 0.5, 'high': coef[0][38] * 1e5 * 1.5},
  {'low':  coef[0][39] * 1e5 * 1.5, 'high': coef[0][39] * 1e5 * 0.5}],
                      initial_population=my_initial_population,
                      gene_type= float,
                      on_generation=my_on_generation)

# Run GA
ga_instance.run()

# Results
best_solutions = ga_instance.best_solutions
solution, solution_fitness, solution_idx = ga_instance.best_solution()
```

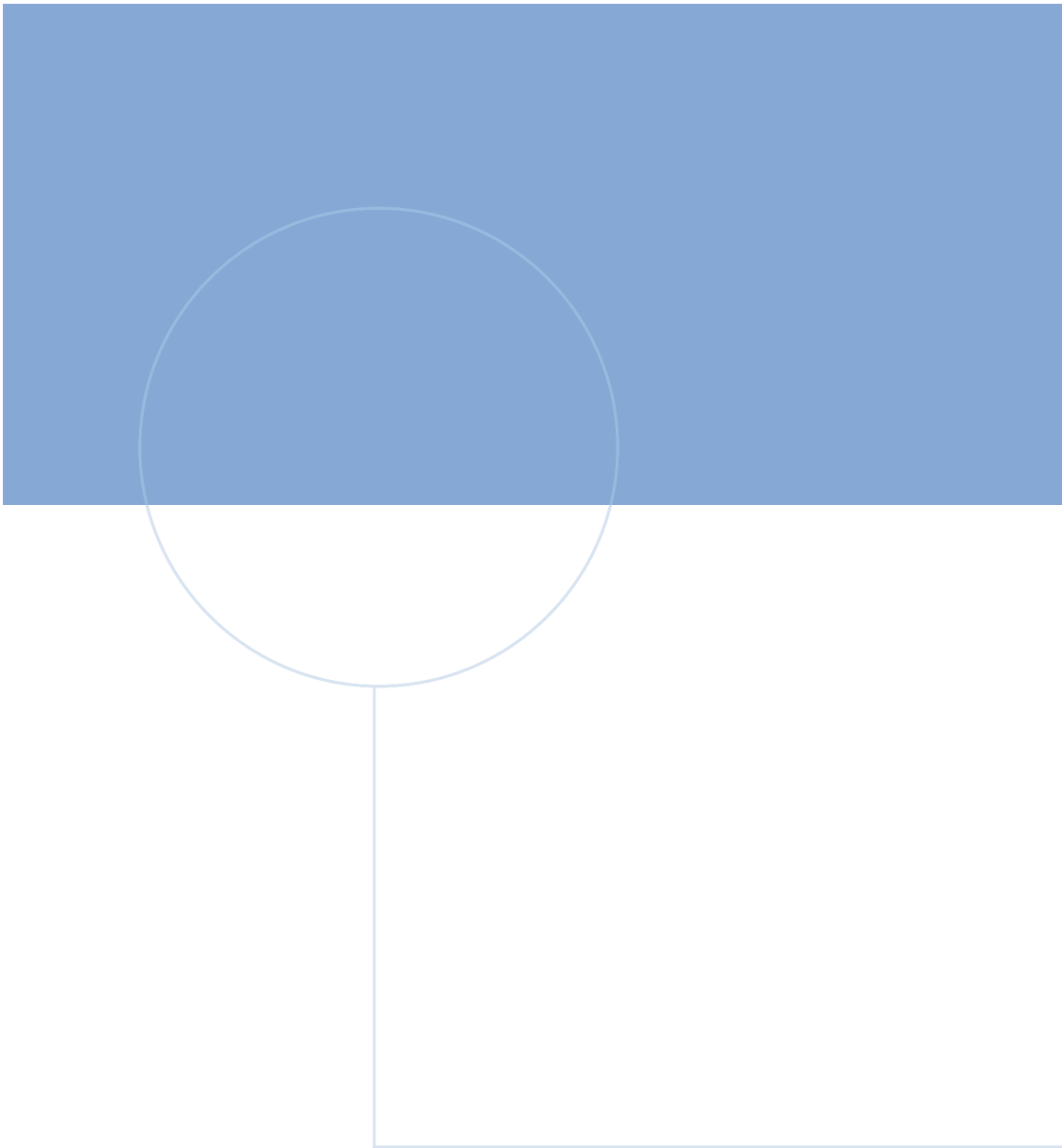

NTNU

Norwegian University of
Science and Technology